Brain, Behavior, and Immunity 123 (2025) 524–539

Contents lists available at ScienceDirect

Brain Behavior and Immunity

journal homepage: www.elsevier.com/locate/ybrbi

Full-length Article

Deleterious effects of social isolation on neuroendocrine-immune status, and cancer progression in rats

Estherina Trachtenberg [a,b], Keren Ruzal [a,b], Elad Sandbank [a,b], Einat Bigelman [a,b], Itay Ricon-Becker [c], Steve W. Cole [c], Shamgar Ben-Eliyahu [a,b], Inbal Ben-Ami Bartal [a,b,*]

[a] School of Psychological Sciences, Tel Aviv University, Tel Aviv, Israel
[b] Sagol School of Neuroscience, Tel Aviv University, Tel Aviv, Israel
[c] Cousins Center for Psychoneuroimmunology, Semel Institute for Neuroscience and Human Behavior, Department of Psychiatry and Biobehavioral Sciences, David Geffen School of Medicine, University of California Los Angeles (UCLA), Los Angeles, CA, USA

A B S T R A C T

Accumulating evidence indicates that social isolation (SI) in humans and rodents is associated with increased cancer incidence and mortality, yet mediating mechanisms remain elusive. Here, we examine the neuroendocrine and immunological consequences of SI and its short- and long-term physiological impacts in naïve and cancer-bearing rats. Findings indicate that isolated animals experienced a significant decrease in weight compared to controls. Specifically, females showed a marked weight decrease during the first week of isolation. Isolated rats had significantly higher numbers of MADB106 experimental pulmonary metastases. Although mortality rates were higher in isolated tumor-bearing rats, unexpectedly, they exhibited a reduced growth rate of orthotopically implanted MADB106 tumors. Transcriptomic analyses of these excised tumors indicated a major downregulation in the expression of various genes, including those associated with pro-metastatic processes (e.g., EMT). In naïve rats (no cancer), levels of IL-6 increased, and total IgG levels decreased under SI conditions. A mixed effect was found for TNFα, which increased in females and decreased in males. In the central nervous system, isolated rats showed altered gene expression in key brain regions associated with stress responses and social behavior. The paraventricular nucleus of the thalamus emerged as a significantly affected region, along with the bed nucleus of the stria terminalis. Changes were observed in the expression of oxytocin, serotonin, and dopamine receptors. Isolated rats also exhibited greater alterations in hypothalamic–pituitary–adrenal (HPA) axis-related regulation and an increase in plasma CORT levels. Our study highlights the profound impact of SI on metastatic processes. Additionally, the potential detrimental effects of SI on thermoregulation were discussed, emphasizing the importance of social thermoregulation in maintaining physiological stability and highlighting the need to avoid single-caging practices in research. We report neuro-immune interactions and changes in brain gene expression, highlighting the need for further research into these underlying processes to improve outcomes in animal models and potential interventions for cancer patients through increased social support.

1. Introduction

Social isolation (SI) and loneliness have profound deleterious impacts on health and are significant risk factors for cardiovascular diseases (Xia and Li, 2018), mental illnesses (Cacioppo et al., 2010), chronic inflammation (Matthews et al., 2024; Uchino et al., 2018), and cancer (Lutgendorf et al., 2020, 2018). The impact of loneliness and SI on morbidity and mortality is comparable to the effects of smoking 15 cigarettes daily (Holt-Lunstad et al., 2015; Wang et al., 2023; Xia and Li, 2018; Yu, 2023). In cancer patients, a few studies addressed mechanisms via which SI can affect pro-metastatic tumor molecular characteristics, such as epithelial-to-mesenchymal transition (EMT). These studies reported associations between SI and pro-metastatic biomarkers, in both ovarian and breast cancer (Bower et al., 2018; Lutgendorf et al., 2020, 2018, 2011).

Rats, like humans, are highly social creatures, and an extensive body of literature demonstrates their sensitivity to SI, which negatively affects their welfare (Begni et al., 2020; de Boer and Koolhaas, 2024), and increases both central and peripheral inflammatory status (Corsi-Zuelli et al., 2019; Dunphy-Doherty et al., 2018; Möller et al., 2013). Similar to the findings in humans, a few studies in rodents have addressed the mediating mechanisms while reporting causal effects on cancer outcomes. SI impacted tumor progression in several studies in mice (Dawes et al., 2020; Madden et al., 2013; Sumis et al., 2016; Villano Bonamin et al., 2001). Only a few studies in rats documented increased mammary tumor progression and/or increased cancer-related mortality (Andrade et al., 2023; Hermes et al., 2009; Hermes and McClintock, 2008; Verza et al., 2021).

In rats, SI is recognized as a mild stressor that affects a wide range of physiological processes, particularly the

* Corresponding author.
E-mail address: inbalbe@tauex.tau.ac.il (I. Ben-Ami Bartal).

https://doi.org/10.1016/j.bbi.2024.10.005
Received 30 July 2024; Received in revised form 20 September 2024; Accepted 5 October 2024
Available online 6 October 2024

hypothalamic–pituitary–adrenal (HPA) axis (Begni et al., 2020; de Boer and Koolhaas, 2024; Fone and Porkess, 2008; Mumtaz et al., 2018). Reduced body weight (BW) is a primary indicator of stress in rodents (de Boer and Koolhaas, 2024), and SI has been shown to decrease BW in both mice and rats (Borges et al., 2023; Hamilton et al., 2022; Sun et al., 2014). The behavioral phenotype in rats indicates that SI increases anxiety-depressive-like behavior and heightens vigilance to other stressors (Du Preez et al., 2020; Fone and Porkess, 2008; Wang et al., 2017).

Brain regions that play a key role in the regulation of stress responses and social behavior, which are also affected by SI, include the amygdala and the bed nucleus of the stria terminalis (BNST) (Conrad et al., 2011; Taugher et al., 2014; Wang et al., 2012). Additionally, the nucleus accumbens (NAc), known for its role in motivation and reward for social interaction, is also affected by SI (Bendersky et al., 2021). Last, the paraventricular nucleus of the thalamus (PVT), though understudied in the context of SI, is extensively interconnected with the above mentioned regions, and may serve as a central hub in mediating stress, social and motivated behavior (Hsu et al., 2014; Iglesias and Flagel, 2021; Penzo and Gao, 2021; Zhou and Zhu, 2019). Despite extensive research into the effects of SI on brain and behavior, the exact neurobiological pathways involved—particularly those influencing peripheral immunity—remain elusive. Understanding their unique biological responses to SI could facilitate new animal-models for SI that may enhance the translation of findings from animal models to clinical testing and implications.

In the current study, we anticipate that social isolation will impact key brain regions and systems associated with stress, social behavior, and motivation. Therefore, we employed a holistic approach, measuring the HPA axis, along with the oxytocin, serotonergic, and dopaminergic systems, which are known to modulate peripheral immune responses (Haykin and Rolls, 2021; Schiller et al., 2021). To achieve this, we measured the gene expression of several receptors within these brain regions that play key roles in these systems. The oxytocin receptor (OXTR), which mediates oxytocin's effects, is involved in social bonding, stress regulation, and can directly impact immune cells (Carter et al., 2020). Recent findings also indicate that oxytocin plays a key role in immune modulation (Jiang et al., 2023; Mehdi et al., 2022). Within the HPA axis, we measured key components of the corticotropin-releasing hormone (CRH) system: CRH receptor 1 (CRH1) and CRH binding protein (CRHBP), which are central regulators of the HPA axis. CRHBP binds and inactivates CRH, while CRH1 mediates CRH's effects (Chu et al., 2024; Herman et al., 2016; Kalin, 2018). 5htr1a is a serotonin receptor involved in regulating mood and stress responses (Garcia-Garcia et al., 2014). Disruptions in serotonin signaling are linked to a range of psychopathologies in humans (Dayer, 2014), and have been specifically associated with anhedonia-like behavior in rats (Li et al., 2022). Lastly, the dopamine receptor 1 (DRD1) plays a critical role in the regulation of motivation and reward, where dopamine is essential for reinforcing behaviors and modulating the reward system (Bromberg-Martin et al., 2010; Frey and McCabe, 2020). Recent studies have also shown dopamine's direct effect on peripheral immune cells (Ben-Shaanan et al., 2016). It has been previously shown that the interaction between these systems is essential for social reward (Dolen et al., 2013). We hypothesize that the interaction of these three systems with the HPA axis is particularly relevant to social isolation, which disrupts both stress and motivation systems.

Our study investigates the effects of SI in rats facing immune challenges, specifically focusing on primary tumor growth and metastasis, while exploring the neuro-immune pathways involved. We hypothesize that SI will adversely affect immunity, exacerbate cancer progression and mortality, and induce central changes in gene expression. Our experimental design includes both short (5 weeks) and long (14 weeks) periods of social isolation in naïve and cancer-bearing rats to investigate these dynamics in the brain and periphery (See Fig. 1).

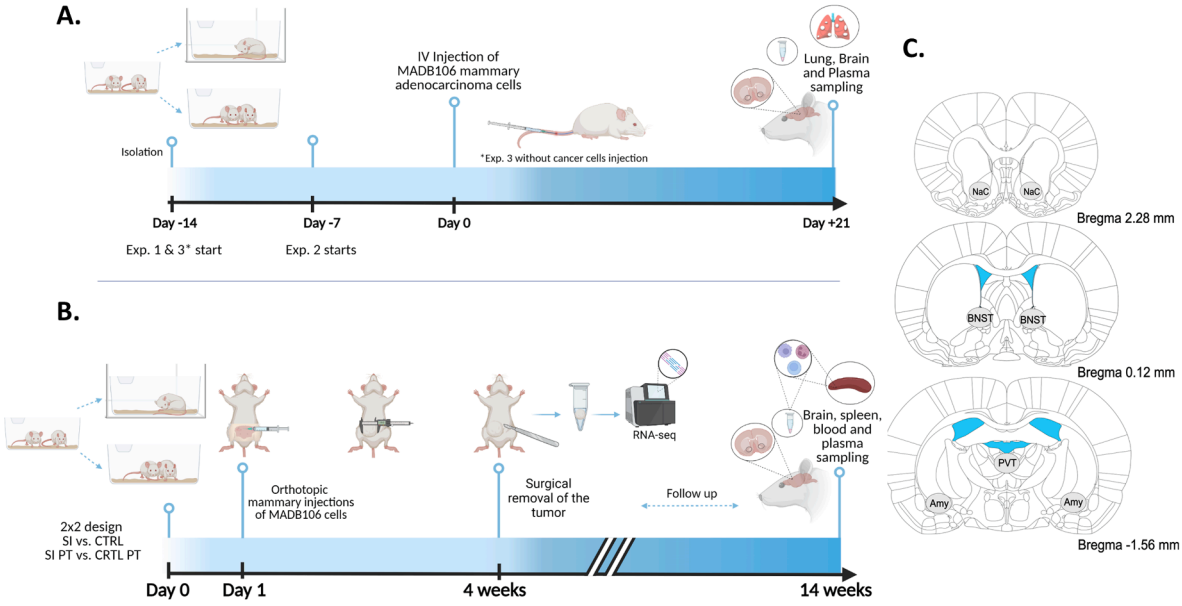

Fig. 1. Experimental timelines (A) Short-term SI up to 5 weeks, w/o the context of metastasis: Exp 1. Isolation was initiated 2 weeks prior to MADB106 cell injection. Exp 2. Isolation was initiated one week prior to MADB106 cell injection. Exp 3. Isolation for 5 weeks with no cancer cell injection. (B) Prolonged (14 weeks) period of SI in naïve and cancer-bearing tumor rats. Exp 4: Isolation was initiated one day prior to orthotopic MADB106 cell injection, and tumors were surgically removed 4 weeks post-injection. Created with BioRender.com (C) Illustrations of the brain regions of interest (ROIs) punches' sites according to the coordinates provided by Paxinos and Watson rat brain atlas (2006).

2. Methods

2.1. Animals

Male and female Fischer 344 (F344) inbred rats (Harlan Laboratories, Jerusalem, Israel), 3–6 months old, were housed 2–4 per cage under standard vivarium conditions, 22 ± 2°C, 12 h light/dark cycle, 50–60 % humidity, with food and water available ad libitum. Rats were lightly handled at the beginning of each experiment to reduce stress during treatment and weighing, which were conducted during the light cycle, from 8 am to 4 pm. All weights at the beginning of each experiment ranged from 200-360 g for males, and 120–200 g for females. Body weight measurements were taken weekly, and changes were reported as a percentage relative to the baseline, which was measured on the first day of the experiment. Age, weight, and sex were evenly distributed across all experimental groups, and in each experiment animals were of similar age. Housing conditions were monitored by the Institutional Animal Care and Use Committee of Tel Aviv University, which also approved all studies described herein (approval numbers: 10–20–006 and TAU-LS-IL-2305–130-5). In Exp. 4 mortality was assessed in PT bearing rats, in SI and CTRL conditions. To assess all-cause mortality (which refers to the total number of deaths from any cause), we monitored the rats every other day and tracked the total number of deaths in each experimental group. A post-mortem investigation was performed to assess the presence of metastases. The mortality rate analysis was calculated using the Chi-square (χ^2) test, based on the death rates within the total number of rats in each group. Humane endpoints were strictly followed: rats that lost more than 20 % of their body weight or appeared to be in severe distress were euthanized to prevent unnecessary suffering and were excluded from the data analysis. Two cases of euthanasia were performed based on these criteria.

2.2. Social isolation

Rats were randomly assigned to either the SI or CTRL groups. Isolated rats were individually housed in cages encased within an opaque plastic barrier in a separate room of the vivarium, with environmental conditions—such as temperature and light—maintained identical to those of the CTRL group. This setup prevented visual contact with other isolated rats and minimized auditory stimuli from non-isolated pairs. For the short-term SI experiment, rats underwent SI for 4–5 weeks. To assess the impact of two weeks of SI on metastasis formation, Exp. 1 initiated SI two weeks prior to the cell line injection (detailed below). In Exp. 2, the SI period was reduced to one week before injection to determine if the same effects occurred over a shorter period. Exp. 3, of similar duration (5 weeks), excluded the cancer context to measure the direct physical effects of SI, with rats remaining in SI or CTRL conditions until the endpoint. For the prolonged period—Exp. 4—we measured the impact of SI on tumor growth, recovery after surgery, and the long-term effects in naïve rats. The total isolation period lasted 14 weeks: 4 weeks for tumor growth and 10 weeks for post-surgery recovery.

2.3. MADB106 tumor cell line

MADB106 is a selected variant cell line derived from a pulmonary metastasis of a chemically induced mammary adenocarcinoma (MADB100) and is syngeneic to F344 rats. Injecting MADB106 into the tail vein induces metastases exclusively in the lungs (Barlozzari, 1985).

2.3.1. Induction of experimental metastases

Rats were lightly anesthetized with 2 % isoflurane, and MADB106 tumor cells in 2.5 ml/kg PBS containing 0.1 % bovine serum albumin (BSA) were injected into their tail vein. Cell dosage was 5 × 10^5/kg (Exp. 1) and 2.5 × 10^5/kg (Exp. 2, to reduce the number of metastases). 21 days later, rats were euthanized, and their lungs were excised and immersed in Bouin's solution for 24 h. The lungs were then rinsed in ethanol, and visible extrapulmonary metastases were counted independently by two experimenters blinded to the experimental groups.

2.3.2. Primary tumor inoculation

To evaluate the effect of SI on orthotopic growth of the PT in females, rats were lightly anesthetized with 2 % isoflurane, and 0.1 × 10^5/kg MADB106 tumor cells in 0.2 ml PBS containing 0.1 % BSA were injected into the left inguinal mammary fat pad. Two weeks post-injection, all PTs were palpable, and 2-weeks later PTs were surgically removed under anesthesia (1.5–2.5 % isoflurane) at an average weight of 5.7 g. Specifically, the area surrounding the PT was shaved and sterilized, followed by an incision around the PT to excise it entirely. The PT developed subcutaneously and did not penetrate the abdominal muscle. The incision was then sutured using 3.0 nylon thread, and the excised PT was weighed and stored at −80 °C for further transcriptomic analyses. Post-mortem inspection revealed no metastases after tumor removal, likely because this cell line does not metastasize spontaneously. Pain alleviation was carried out through paracetamol administration (250 mg/kg) for the three days following surgery.

2.4. Peripheral immune-neuroendocrine assays

2.4.1. Plasma analytes

Rats were euthanized by an overdose of isoflurane, and blood was collected from the left atrium of the heart within a maximum of 3.5 min of approaching the animals, using EDTA-coated syringes. Blood was then centrifuged at 1000g at 4 °C for 20 min, and plasma was collected and stored in aliquots at −20 °C until further analyses.

To measure pro-inflammatory cytokine levels, we chose the standard key parameters IL-6 and TNFα, which were widely used (Smith et al., 2020) and available in sensitive and high-quality kits for rats. These kits enabled accurate measurement of these cytokines even without immune challenges in our hands. We selected plasma IgG levels as a general indicator of immune system function. This measure is used to assess the organism's ability to produce antibodies and its overall immune response capacity (Schroeder and Cavacini, 2010). Immunosorbent assay (ELISA) kits were used in duplicate to assess plasma levels of corticosterone (CORT) (EC3001, AssayPro, St. Charles, MO, assay range: 0.391——100 ng/ml) and TNFα and IL-6 (RTA00 assay range: 12.5——800 pg/mL, sensitivity 5 pg/mL, R6000B assay range 62.5——4,000 pg/mL, sensitivity 36 pg/mL, R&D Systems, Minneapolis, MN), according to the manufacturer's protocol. To increase the detectability of the two cytokines, plasma was diluted by 1.5-fold, rather than by 2-fold, based on consultation with R&D Systems Technical Support.

For assessing total plasma IgG, 96-well plates were coated with 2 μg/mL Anti-Rat IgG Fc ab125900 (Abcam) and incubated overnight at 4 °C. Plates were then blocked with a blocking buffer (3 % BSA 0.05 % Tween 20 mM EDTA) for 2 h at room temperature, then washed with 0.05 % Tween PBD (PBST). Plasma samples were diluted by 1:819200 in the blocking solution, and 60 μl of diluted plasma was incubated in each well of the plate for 1 h at room temperature. Following a PBST wash, plates were incubated with horseradish peroxidase (HRP)-conjugated anti-rat IgG secondary antibody BLG-405405 (0.16 μg/mL, Biolegend) for 45 min at room temperature, and then rewashed. After washing, TMB ab171523 (Abcam) was added, and the optical density (OD) of the plates was read at 650 nm. All ELISA analyses were performed using the Multiskan™ FC (Thermo Scientific).

2.4.2. Splenic and whole blood leukocytes isolation

Upon euthanasia, blood was collected from the left atrium of the heart using EDTA-coated syringes and immediately placed on ice. Spleens were carefully excised and submerged in cold phosphate-buffered saline (PBS) on ice until further processing. Red blood cells (RBCs) from the collected samples were lysed using a 1:10 dilution of RBC lysis buffer (155 mM NH4Cl, 10 mM KHCO3) and incubated for 5 min at room temperature. Samples were then centrifuged at 400g for 5

min at 4 °C. The supernatant was discarded, and the cell pellet was washed once with PBS (1:10 dilution) before a second centrifugation under the same conditions. Finally, the cell pellet was resuspended in NutriFreez® D10 Cryopreservation Media (Sartorius) and stored at −80 °C. Spleen tissues were homogenized using a pestle (Biofil), passed through a 70 μm cell strainer (Corning), and centrifuged at 400g for 5 min at 4 °C. RBCs were lysed as previously described, and the samples were washed with PBS, followed by centrifugation at 400g for 5 min at 4 °C. The final cell pellet was resuspended in NutriFreez® D10 (Sartorius) and frozen at −80 °C for subsequent analysis.

2.4.3. Flow cytometry

For flow cytometry analysis, all samples containing leukocytes from spleen and whole blood were rapidly thawed in warm RPMI 1640 medium supplemented with 10 % fetal bovine serum (FBS) (Thermo Fisher Scientific) and maintained at 37 °C. After thawing, samples were centrifuged at 400g for 5 min at 4 °C. Cell pellets were resuspended in cell staining buffer (FC control, BLG420201) and stained with fluorescence-conjugated monoclonal antibodies for 30 min at 4 °C in the dark. The following antibodies were used: anti-rat CD3 (BLG-201403) to gate T-cells, anti-CD4 (BLG-201403), anti-CD8 (BLG-200610), and anti-CD25 (BLG-202105). Additional markers included anti-CD45RA (MCA340FT), anti-CD161 (BLG-205604), and anti-CD11b/c (BLG-201809) from Biolegend and Bio-Rad. Cell viability was assessed using 7-AAD viability staining (Thermo Fisher 00–6993), with all samples achieving 85 % or greater viability. Flow cytometry was conducted using the CytoFLEX S2 instrument (Beckman Coulter, Brea, CA, USA), and data were analyzed using FlowJo software.

2.5. Brain dissection and punches

Upon euthanasia, brains were removed and snap-frozen on dry ice, then stored at −80 °C until slicing. The tissue was sliced in a coronal orientation on a cryostat. Tissue was obtained from each hemisphere using a 1 mm diameter Miltex biopsy puncher (Bar Naor, Israel), aimed for real-time quantitative polymerase chain reaction (PCR) analysis. Punches were taken directly while the brain was on the cryostat, the thickness of each punch 0.7–1 mm (measured by the number slices rotated in the cryostat). Four brain regions of interest (ROIs) were collected: the NAc, amygdala, BNST, and PVT. According to the coordinates provided by Paxinos and Watson rat brain atlas (2006): NAc: 2.28—–1.20 mm, BNST: 0.12 − −0.96 mm, amygdala and PVT −1.56 − −2.92 mm (See Fig. 1C). All tissue punches were immediately frozen on dry ice after collection and stored in clean tubes at −80 °C until rtPCR analysis.

2.6. Quantitative real-time polymerase chain reaction (rtPCR)

Total RNA was first isolated with Trizol (Thermo Scientific) and chloroform (Sigma-Aldrich Israel Ltd.). Subsequently, 250 ng of RNA per reaction was reverse transcribed into cDNA using the Verso cDNA Kit (Thermo Scientific). The quantitative real-time PCR (rtPCR) was conducted using a Fast SYBR Green PCR Master Mix (Applied Biosystems) along with specific primers for *Oxtr* and *Gapdh* genes (HyLabs Israel Ltd.) (See primers sequences in Supplementary table 1S). To standardize gene expression levels, all genes were normalized to *Gapdh*, which was used as the reference gene for rtPCR based on its application in previous studies involving similar manipulations, such as isolation in rats and assessment of brain tissues (Panossian et al., 2020; Wang et al., 2017). *Gapdh* exhibited stable expression across our experimental conditions, with no significant differences between the SI and CTRL groups ($t(_{190}) = 0.17$, $p = 0.43$). Product purity was validated through a melt curve analysis using ABI hardware and software (QuantStudio Real-Time PCR Systems, Thermo Scientific), and gene expression analyses were determined using the comparative ΔΔCt (fold change) method.

2.7. Primary tumor RNA sequencing (RNA-seq)

Tumors were snap-frozen upon excision and subject to genome-wide transcriptional profiling in the UCLA Social Genomics Core Laboratory as previously described (Haldar et al., 2023). Briefly, RNA was extracted from approximately 2 g of frozen tumor tissue (Qiagen RNeasy), assessed for suitable mass (RiboGreen), reverse transcribed to cDNA using a high efficiency mRNA-targeted enzyme system (Lexogen QuantSeq 3′ FWD) and subsequently sequenced using Illumina NovaSeq instrument (Lexogen Services, GmbH). Sequencing targeted 10 million sequencing reads per sample (achieved mean = 14.5 million) each of which was mapped to the mRatBN7.2 genome sequence (average 99 % mapping rate) and normalized to transcripts per million using the STAR aligner.

2.7.1. Bioinformatic analysis

RNA-seq bioinformatics analysis was performed using R (version 4.1.1). Log2-transformed transcript abundance values were used as input for standard linear models to assess the magnitude of differences in gene expression between groups (SI vs. control). Genes showing ≥ 2-fold difference in response to SI (vs. control), were used as input for higher level bioinformatic analysis using the Transcription Element Listening System (TELiS, http://www.telis.ucla.edu/) (Cole et al., 2005). The TELiS analysis focused on activity of a-priori defined transcription factors implicated in pro-inflammatory/anti-tumor pathways (NF-κB, CREB, GR), hypoxic response (HIF1, HIF2a), and metabolic processes (FOXO3, FOXO4). Additionally, the Transcript Origin Analysis (TOA) method was employed, using established reference gene profiles from the Gene Expression Omnibus to assess epithelial-to-mesenchymal transition (EMT) (GSE13915 (Choi et al., 2010)), leukocyte subsets (GSE1133 (Su et al., 2004)), and M1-M2 macrophage polarization (GSE5099 (Martinez et al., 2006)). For all bioinformatics analyses, statistical significance was assessed from standard errors derived by bootstrap resampling of linear model residual vectors across genes (200 cycles). This approach controls for any statistical dependence among genes (Cole et al., 2005; Powell et al., 2013).

2.8. Statistical analysis

Statistical analyses were conducted to compare different experimental groups. Comparisons were made using a Student's *t*-test (two-tailed) or one- or two-way analysis of variance (ANOVA). For variables measured repeatedly, such as percentage body weight (%BW), a repeated measures ANOVA was employed. All tests were set at a predetermined significance level of 0.05. In cases where significant differences between groups were detected, Fisher's protected least significant difference (Fisher's PLSD) test was applied for pairwise post hoc comparisons. All means are reported as mean ± SEM. Statistical computations were performed using SPSS v29 or GraphPad PRISM v10 software.

3. Results

3.1. Experiments 1 & 2: Short-term effects of SI on body weight and lung metastases

Two separate experiments were conducted. In Exp. 1 (n = 19 males, n = 21 females), F344 rats were subjected to SI for 2 weeks prior to I.V. MADB106 cell injection or remained with their counterparts in their home cage (CTRL). Following tumor cell inoculation, SI was maintained for an additional 3 weeks until all rats were euthanasiad for harvesting lungs and blood tissues. In Exp. 2 (n = 12 males, n = 12 females), one week of SI was employed before tumor cell injection, and the procedure of Exp. 1 was followed (Fig. 1A).

3.1.1. Body weight

SI significantly reduced Body weight (BW) in both experiments, in a

sex- and time-dependent manner. In Exp. 1, significantly lower %BW was observed in the SI condition compared to ctrl SI (repeated measures ANOVA: $F_{(1, 36)} = 16.1$, $p < 0.001$), with a significant main effect of sex ($F_{(1, 36)} = 8.7$, $p = 0.006$), but no interaction between SI and sex ($p > 0.05$). (Fig. 2A). Analysing specifically the %BW change at the end of the first week of SI, two-way ANOVA (SI by sex) revealed a significant effect of SI ($F_{(1, 36)} = 16.5$, $p < 0.001$), and post-hoc LSD (PLSD) indicated a significantly greater reduction in %BW in isolated females compared to isolated males ($p = 0.03$). (Fig. 2B). In Exp. 2, similar to Exp. 1, SI significantly reduced BW (repeated measures ANOVA: $F_{(1, 20)} = 6.0$), loss was observed in all groups post tumor injection. SI females exhibited a significant reduction in %BW following tumor injection compared to CTRL females (PLSD, $p = 0.014$) (Fig. 2D).

3.1.2. MADB106 experimental metastases

Two weeks of SI prior to tumor injection (Exp. 1) significantly increased the number of lung metastases compared to CTRL (75 ± 27 vs. 47 ± 24, $F_{(1, 36)} = 10.7$, $p = 0.002$) (Fig. 2E), while no significant effects were observed in sex or sex by SI interaction ($p > 0.05$). One week of SI prior to cell injection (Exp. 2) resulted in a similar pattern of outcomes (34 ± 19 vs. 21 ± 12, $F_{(1, 22)} = 4.17$, $p = 0.055$) (Fig. 2G). When examining corticosterone plasma levels at the time of lung harvest in Exp. 2, no significant difference was identified between the SI and CTRL groups (CTRL 681 ± 871 ng/ml vs. SI 906 ± 1200 ng/ml). However, a significant correlation between corticosterone levels and the number of lung metastases was observed ($R^2 = 0.201$, $p = 0.028$).

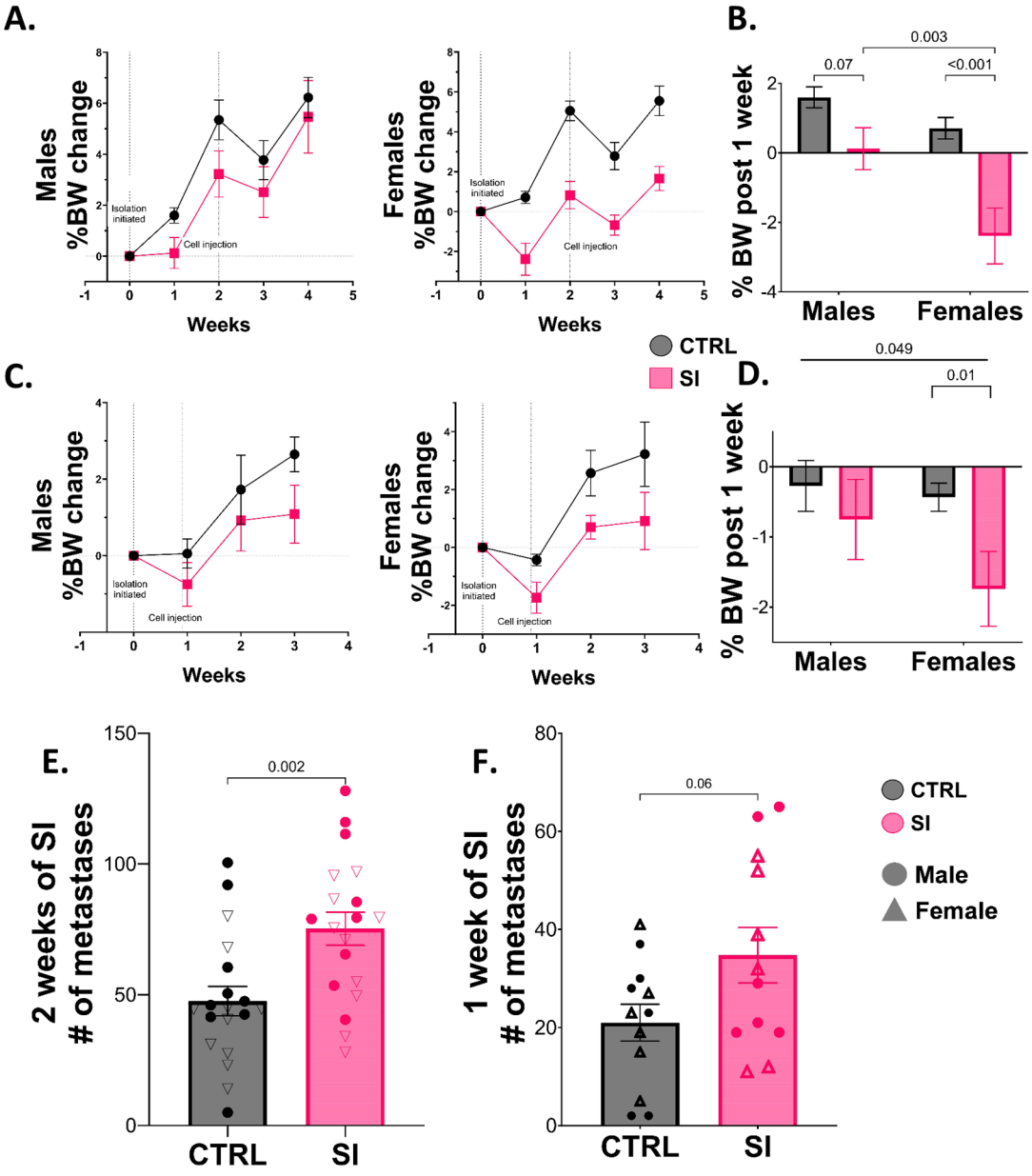

Fig. 2. The effect of SI on body weight and lung metastases. (A-D) Relative change in body weight at weekly time points throughout the experimental period. Bar graphs showing the change in %BW after the first week of SI. (A-B) Exp 1. (C-D) Exp 2. (E-F) Mean number of metastases after two weeks (Exp 1.) and one week (Exp 2.) of SI prior to cell injection. All error bars represent the standard error of the mean (SEM).

3.2. Experiment 3: Short-term effects of SI on neuroendocrine status in naïve rats

Female and male F344 rats remained in their home group cage or were isolated for 5 weeks before being euthanasiad for collection of blood and brain tissues (Fig. 1A) (n = 34 males, n = 36 females). Different animals were used to assess different indices, as detailed below.

3.2.1. Body weight, CORT, cytokines, and IgG levels

Consistent with previous findings, SI significantly reduced %BW (repeated measures ANOVA: $F_{(1, 58)} = 13.4$, $p < 0.001$), with an approaching significance effect of sex ($F_{(1, 58)} = 3.06$, $p = 0.056$) and no significant interaction effect (Fig. S1). Focusing on %BW at the end of the first week of SI, a two-way ANOVA (SI by sex) revealed a significant effect of SI ($F_{(1, 58)} = 7.1$, $p = 0.01$). PLSD indicated a significantly greater reduction in %BW in SI females compared to CTRL females ($p = 0.02$), while no significant effect was observed in SI males ($p > 0.05$). Plasma CORT levels were significantly higher in the SI condition ($F_{(1, 68)} = 7.2$, $p = 0.009$), with a trend toward a sex effect ($F_{(1, 68)} = 3.06$, $p = 0.08$) and a significant sex by SI interaction ($F_{(1, 68)} = 3.8$, $p = 0.05$), indicating a larger increase in CORT levels in females compared to males. PLSD contrasts showed a significant increase in CORT levels in SI females compared to CTRL females ($F_{(1, 36)} = 7.6$, $p = 0.009$), while no significant changes were observed in males ($p < 0.05$) (Fig. 3A). For the assessment of plasma levels of TNFα, IL-6, and IgG, 3–7 animals per group were randomly chosen (separately for each index), as seen in Fig. 3B-F. No significant effects in plasma TNFα levels were observed for SI ($p > 0.05$). However, a significant interaction between sex and SI was revealed ($F_{(1, 26)} = 26.1$, $p < 0.001$), with PLSD contrasts showing a significant increase in isolated females ($p < 0.001$) and a significant decrease in isolated males ($p = 0.003$) (Fig. 3B). Plasma IL-6 levels were elevated in isolated rats, approaching significance ($F_{(1, 10)} = 4.8$, $p = 0.052$), with no effects for sex or interaction ($p > 0.05$) (Fig. 3C). SI significantly decreased total plasma IgG levels ($F_{(1, 21)} = 8.04$, $p = 0.01$), with no significant effect for sex ($p > 0.05$), but with a significant sex by SI interaction ($F_{(1, 21)} = 14.5$, $p = 0.001$). PLSD indicated a significant decrease in males ($p = 0.003$) and a non-significant increase in females ($p = 0.37$) (Fig. 3D). Assessing the correlations between CORT and the three plasma indices revealed a significant negative correlation between IL and 6 and CORT levels ($R^2 = 0.373$, $p = 0.02$) (Fig. 3E).

3.2.2. Changes in Oxtr, Crhbp, Crh1, 5htr1a and Drd1 gene expression in the NAc, BNST amygdala and PVT in isolated naïve rats

To examine the neuromodulatory effects of SI, several genes of interest were quantified in brain regions associated with social behavior. This analysis revealed significant differences in gene expression between conditions across tested regions. As significant differences between males and females were observed in the control condition (Fig. S2), all analyses were conducted separately for males and females.

In the NAc, *Oxtr* expression was significantly higher in SI females compared to CTRL ($F_{(1,7)} = 3.8$, $p = 0.03$), but not in males. However, a trend toward increased *Crhbp* expression was noted ($F_{(1,8)} = 4.9$, $p = 0.057$) (Fig. 4A). In the BNST, SI females demonstrated a significant increase in both *Crh1* and *Crhbp* expression ($F_{(1,7)} = 48.5$, $p < 0.001$ and $F_{(1,7)} = 69.1$, $p < 0.001$, respectively), along with an approaching significance in *5htr1a* expression ($F_{(1,7)} = 5.3$, $p = 0.053$) (Fig. 4B). Conversely, SI males exhibited a trend toward a decrease in in *Drd1* expression ($F_{(1,8)} = 4.6$, $p = 0.07$) (Fig. 4C). In the amygdala, SI females showed a significant decrease in *Crhbp* expression ($F_{(1,7)} = 7.5$, $p =$

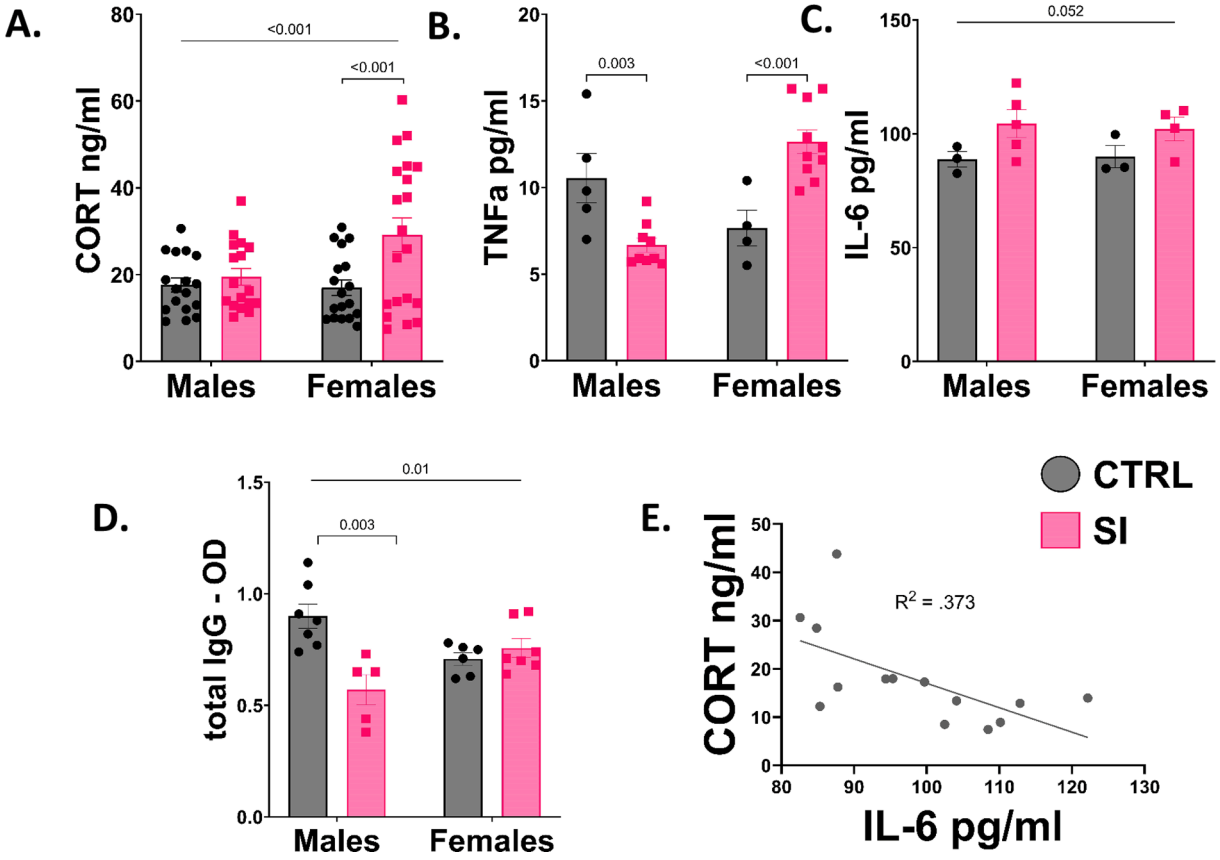

Fig. 3. The effect of SI on plasma CORT, TNFα, and total IgG levels in naïve rats – Exp 3. (A) Corticosterone (CORT) ng/ml levels. (B) TNFα levels pg/ml. (C) IL-6 pg/ml levels. (D) Total IgG optic density values. (E) Correlation between CORT and IL-6 levels.

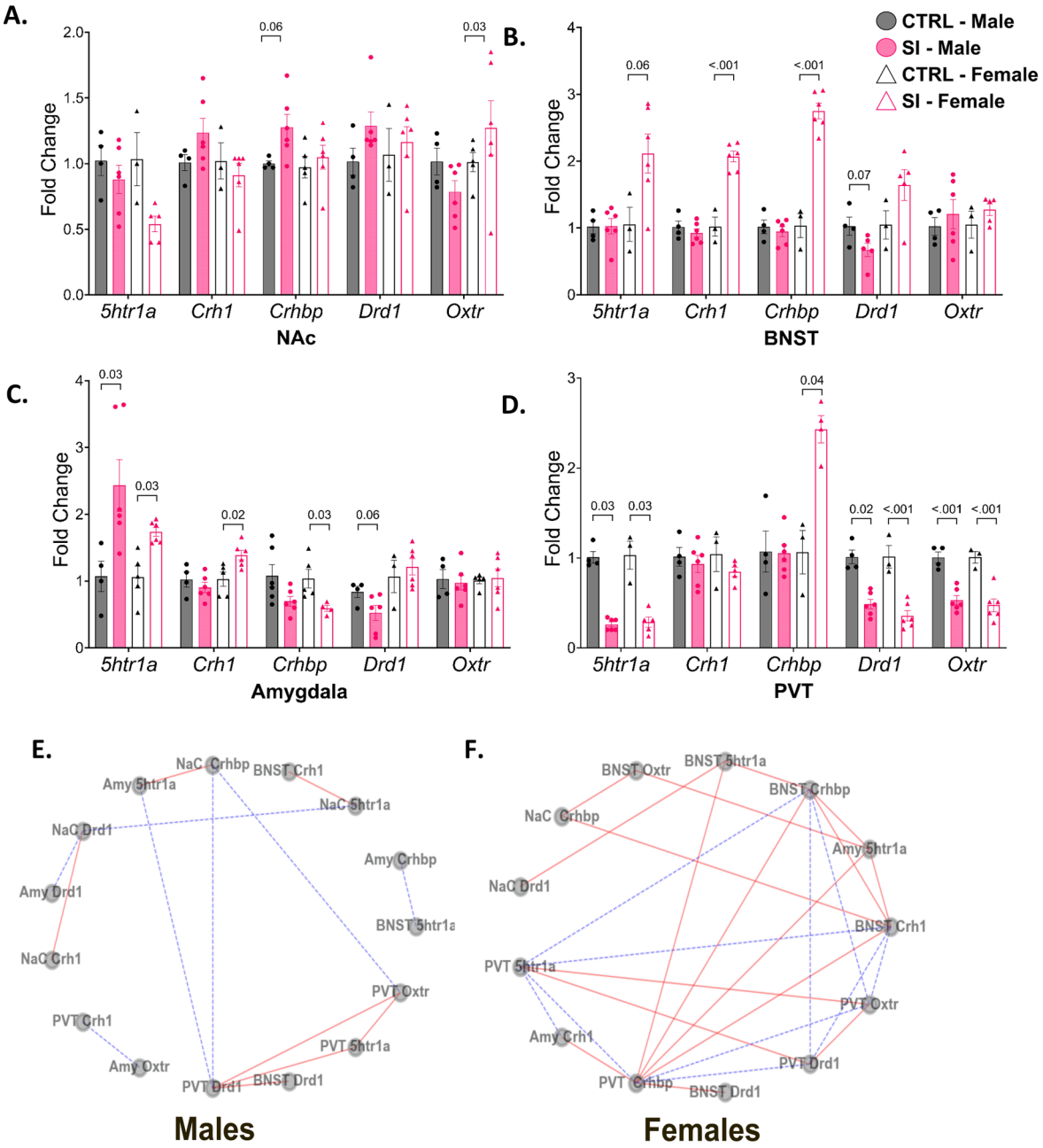

Fig. 4. The effect of SI on gene expression in the NAc, BNST, Amygdala, and the PVT in naïve rats – Exp 3. (A) Nucleus accumbens (NAc). (B) Bed nucleus of the stria terminalis (BNST). (C) Amygdala. (D) Paraventricular thalamus (PVT). (E-F) Correlation between gene expression and 4 other regions, represented here only for r > 0.7 and significant at p < 0.05, blue dashed lines represent negative correlations, red lines represent positive correlations. (For interpretation of the references to colour in this figure legend, the reader is referred to the web version of this article.)

0.03), and significant increases in *Crh1* and *5htr1a* expression ($F_{(1,9)} = 7.5$, $p = 0.02$; $F_{(1,9)} = 16.9$, $p = 0.03$, respectively) (Fig. 4D), while SI males exhibited a significant increase in *5htr1a* expression ($F_{(1,8)} = 6.8$, $p = 0.03$) (Fig. 4E). In the PVT, a similar pattern was observed in both SI females and males, with significant decreases in *5htr1a*, *Drd1*, and *Oxtr* gene expression ($F_{(1,7)} = 29.2$, $p = 0.02$; $F_{(1,8)} = 149.6$, $p < 0.001$; $F_{(1,7)} = 30.9$, $p < 0.01$; $F_{(1,8)} = 33.4$, $p < 0.001$; $F_{(1,7)} = 22.6$, $p = 0.02$; $F_{(1,8)} = 34.4$, $p < 0.001$, respectively). Additionally, a significant increase in *Crhbp* expression was documented in SI females ($F_{(1,5)} = 25.8$, $p = 0.04$) (Fig. 4D).

To determine whether certain genes were functionally connected, network analysis was conducted across all genes and brain regions for males and females separately. To this end, a correlation matrix was constructed based on Pearson's correlations for the fold change values (Fig. S3), and network graphs were created displaying the top correlations thresholded at 0.7 (Fig. 4E-F). This analysis revealed that females had a significantly higher number of significant correlation networks than males ($t_{(30)} = 1.9$, $p = 0.01$). Moreover, the PVT emerged as a central hub in males and females with the highest number of coefficient degrees (Fig. 4E-F).

3.3. *Experiment 4: Prolonged SI in the context of a primary tumor – Immune and neuroendocrine effects*

To examine the effects of long-term isolation on the immune system, adult female F344 rats were isolated for 14 weeks or remained in their

home group cages. In a two-by-two design, rats were randomly assigned to one of four groups: SI or CTRL, with or without a primary tumor (PT) (n = 58). On the second day of SI, rats in the PT groups received orthotopic mammary injections of MADB106 cells, and a month later tumors were surgically removed. Ten weeks post-PT removal, all animals were euthanized, and spleen, blood, and brain tissues were collected (Fig. 1B).

3.3.1. Body weight and mortality rate

A 2 x 2 repeated measures ANOVA indicated that across the 14-week period, bearing a PT and its removal significantly reduced %BW ($F_{(1, 44)} = 60.5$, $p < 0.001$). SI significantly reduced %BW ($F_{(1, 44)} = 4.1$, $p = 0.04$), and no significant interaction was observed ($p > 0.05$) (Fig. 5A-B). On day seven of SI, the SI-PT group exhibited a significantly greater reduction in %BW than the other three groups (PLSD, $p < 0.01$). At the end of the experiment (14 weeks), the all-cause mortality rate among the SI-PT group was significantly higher than that in the CTRL-PT group, (8 vs. 2 rats; X^2 (1,34) = 3.9, $p = 0.04$) (Fig. 5C). The all-cause mortality rate was summed at the end of the experiment for each group; for full individual representation (Fig. 5D).

3.3.2. MADB106 primary tumor weight and gene expression

Upon excision, PTs were weighed and frozen to assess the effect of SI on MADB106 tumor weight and transcriptomics. Surprisingly, isolated rats had significantly reduced PT weight compared to CTRL rats ($F_{(1,37)} = 2.5$, $p = 0.015$). (Fig. 6A). Primary analysis of PT whole-genome RNA transcripts indicated that SI upregulated 292 genes > 2-fold and downregulated 4,811 genes by the same magnitude (see the volcano plot, Fig. 6B). A follow-up bioinformatic analysis of EMT among these DEGs indicated a significant reduction in EMT in PTs from SI rats (vs. control), as indicated by increased expression of genes associated with epithelial differentiation (0.246 ± 0.07, p = 0.002) (Fig. 6C). Additionally, SI significantly altered M1/M2 polarization in SI rats (vs. control), as indicated by a significant downregulation of M2-related genes (0.251 ± 0.10, p = 0.013) (Fig. 6C). TOA analyses examining transcriptional activity associated with tumor-infiltrating leukocytes (TILs) subpopulations in the PTs of SI rats (vs. control) found SI-upregulated genes derived predominately from CD8 + T-cells (0.367 ± 0.07, $p < 0.001$), B-cells (0.641 ± 0.08, $p < 0.001$), NK cells (0.146 ± 0.05, $p < 0.01$), and neutrophils (0.410 ± 0.15, $p < 0.01$) (Fig. 6D). TELiS promoter-based bioinformatic analysis comparing SI and CTRL indicated reduced transcriptional control activity of CREB (mean log ratio = -0.732 ± 0.130, $p < 0.001$), HIF1a and HIF2a (−0.662 ± 0.133, $p < 0.001$; −0.378 ± 0.100, $p < 0.001$, respectively), and NF-kB (−0.276 ± 0.103, $p < 0.01$). This was accompanied by increased activity of the FOXO3 and FOXO4 transcription factors (0.441 ± 0.207, p = 0.03; 0.462 ± 0.100, p = 0.05, respectively) and the glucocorticoid receptor (GR) (0.145 ± 0.046, $p < 0.001$) (Fig. 6E).

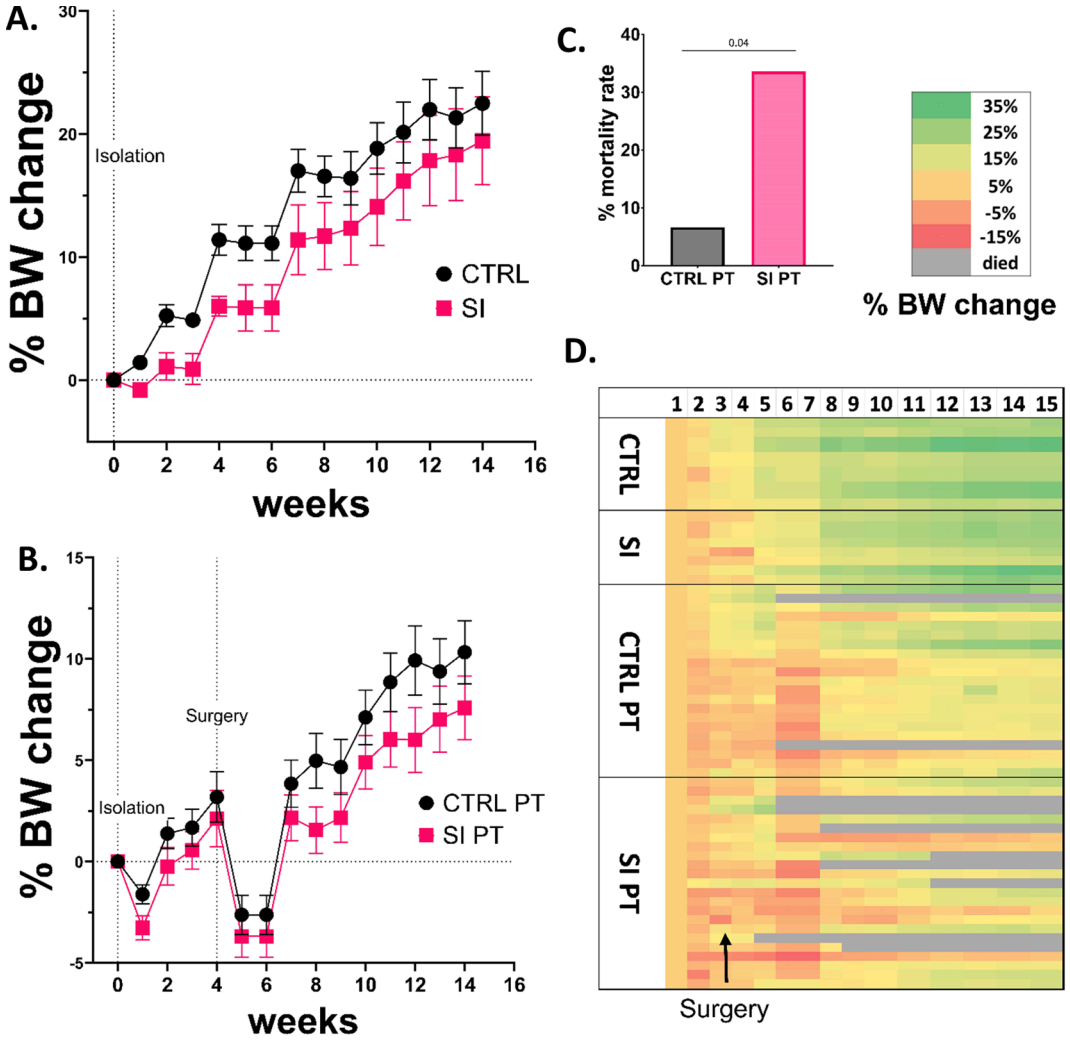

Fig 5. The effect of long-term SI on body weight and mortality in tumor-bearing and naïve rats Exp 4. (A-B) Relative change in body weight at weekly time points throughout the experimental period. (C) Percentage of all-cause mortality rate in tumor-bearing rats. (D) Individual representation of weekly changes in the percentage of body weights or mortality in grey, throughout the 14 weeks of the experiment.

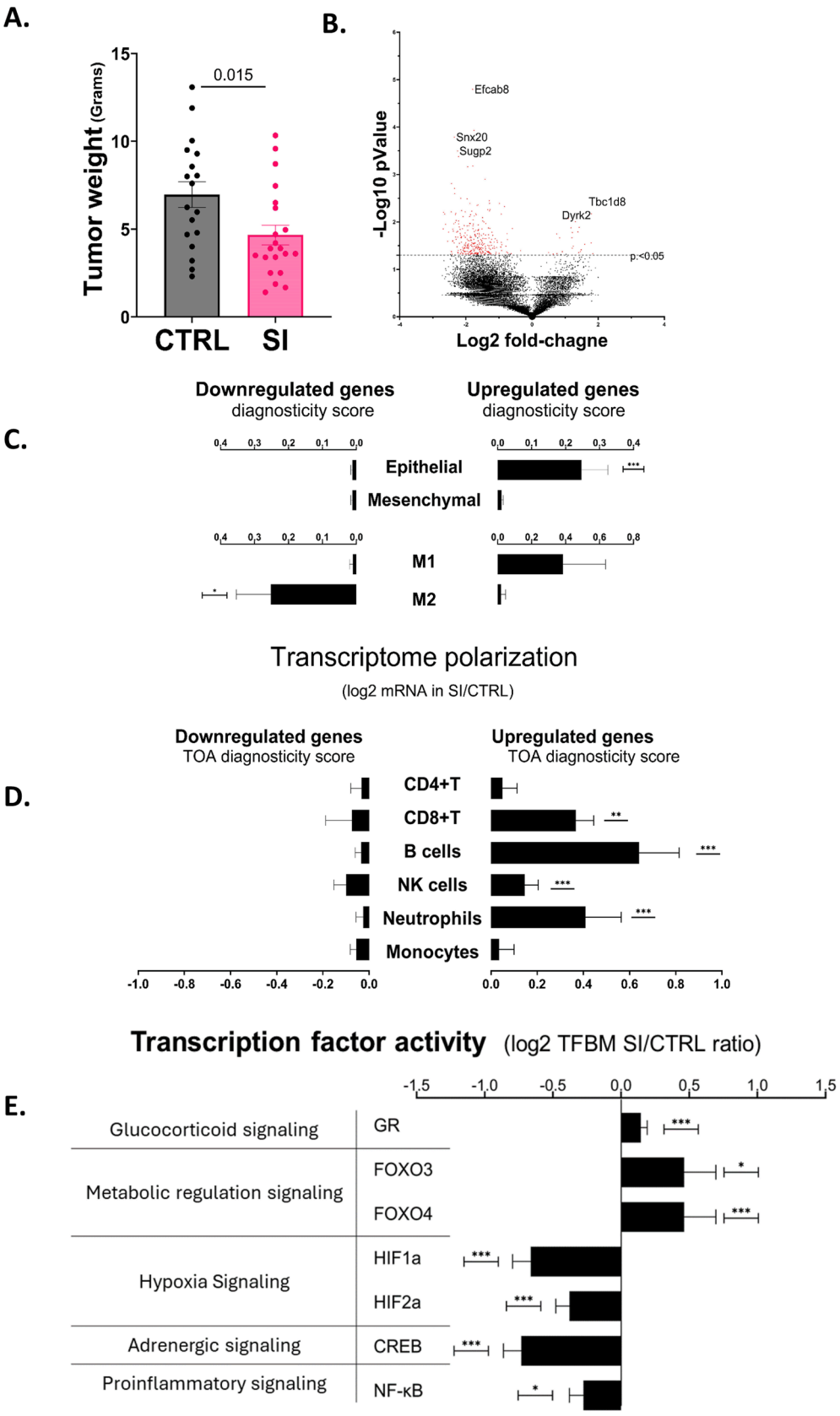

Fig 6. The effect of four weeks of SI on molecular characteristics of the primary tumors. (A) Tumor weights in grams. (B) Volcano plots of differentially expressed genes (DEG) in SI vs. CTRL. (C) Epithelial-to-mesenchymal transition (EMT) and M1-M2 polarization. (D) Transcript origin analysis (TOA) of the cellular sources of the SI-DEG indicative of neutrophils, monocytes, NK cells, T cells, and B cells. (E) Activity of transcription control pathways based on analyses of transcription factor binding motifs (TFBMs) in promoters of differentially expressed genes. *p < 0.05, **p < 0.001, ***p < 0.0001.

3.3.3. Plasma TNFa, CORT and IgG levels

Plasma was collected at the end of the 14-week follow-up period. TNFα levels were assessed only in the PT groups and were found to be significantly higher in SI compared to CTRL animals ($F_{(1,8)} = 3.9$, $p = 0.004$) (Fig. 7A). A two-way ANOVA (PT by SI conditions) of all other measures was conducted. Total IgG levels were significantly lower in SI rats ($F_{(1,17)} = 8.5$, $p = 0.01$), with no significant effect of PT ($p > 0.05$) or PT by SI interaction ($p > 0.05$) (Fig. 7B). No significant effect of SI or PT was observed in plasma CORT levels ($p > 0.05$) at this time point.

3.3.4. Splenic and circulating immunocytes

Splenic and blood leukocyte subpopulations were identified by flow cytometry, including NK cells (CD161 +), B cells (CD45Ra +), CD8 and CD4 T cells, and CD11b/c + cells (monocytes, granulocytes, macrophages). Two-way ANOVA indicated that PT significantly increased the percentage of splenic CD161+/NK cells ($F_{(1,21)} = 7.4$, $p = 0.012$), with no significant effect of SI or PT-SI interaction ($p > 0.05$) (Fig. 7C). Conversely, in the blood, PT significantly decreased the percentage of CD161+/NK cells ($F_{(1,17)} = 8.01$, $p = 0.012$), with no significant effect of SI or interaction ($p > 0.05$) (Fig. 8D). SI significantly decreased the percentage of blood CD11b/c + cells ($F_{(1,17)} = 7.4$, $p = 0.014$), with a trend toward a decrease caused by PT ($F_{(1,17)} = 4.0$, $p = 0.06$), and no significant PT-SI interaction ($p > 0.05$) (Fig. 8E). No significant effects were observed in the other immunocytes examined. A significant negative correlation was found between blood %NK cells and PT weight ($R^2 = 0.583$, $p = 0.02$) (Fig. 7F), although PT weights were assessed 10 weeks earlier.

3.3.5. Changes in Oxtr and Crh1 gene expression in the NAc, BNST amygdala and PVT in the context of PT during SI

To assess the main effects of SI and PT on gene expression in the four brain regions, a 2 x 2 ANOVA was conducted. In the NAc, SI significantly decreased *Oxtr* expression ($F_{(1,15)} = 4.8$, $p = 0.045$) alongside a with a trend toward a decrease caused by PT ($F_{(1,15)} = 3.5$, $p = 0.07$), with no significant interaction effect detected ($p > 0.05$) (Fig. 8A). In the BNST, SI significantly increased *Crh1* expression ($F_{(1,14)} = 4.4$, $p = 0.05$), with no effect for PT or SI-PT interaction ($p > 0.05$) (Fig. 8B). *Crh1* expression in the PVT showed a significant SI-PT interaction effect ($F_{(1,15)} = 5.6$, $p = 0.031$), but no effect of PT or SI alone ($p > 0.05$) (Fig. 8C). In the amygdala, no significant alterations were observed in any genes across all conditions.

Pearson correlation across all four brain ROIs and gene expressions was conducted, showing that the amygdala had high internal correlations ($r > 0.7$). Similarly to previous results in females in the short-term SI experiment, the PVT was highly correlated with other regions. For instance, *Oxtr* in the PVT was positively correlated with *Crh1* in the amygdala ($r = 0.632$, $p = 0.006$) and *5htr1a* in the PVT ($r = 0.638$, $p = 0.004$) was positively correlated with *Crhbp* in the amygdala ($r = 0.650$, $p = 0.001$). See Fig. S4 for the full correlation matrix.

3.3.6. OXTR, Crhbp mRNA levels correlate with CORT plasma levels

Although no significant differences were found in CORT levels between the four groups, significant correlations between plasma CORT levels and mRNA levels from the brain regions were identified. CORT was positively correlated with *Oxtr* in the NAc and in the amygdala ($r = 0.452$, $p = 0.04$; $r = 0.410$, $p = 0.052$), and negatively with *Crhbp* in the BNST ($r = -0.450$, p 0.03). Apart from these, no other correlations between CORT and gene expressions in the brain were found (Fig. 8C).

4. Discussion

This study explored the impact of isolation on rats. Consistent with our hypothesis, we observed an increase in susceptibility to lung metastasis following one or two weeks of SI prior to inoculation of the cell line. This aligns with literature findings that have linked SI with cancer progression in rats (Andrade et al., 2023; De la Roca-Chiapas et al., 2016; Hermes et al., 2009; Hermes and McClintock, 2008; Verza et al., 2021). Notably, our research is the first to demonstrate that SI can exacerbate experimental metastases, indicating reduced host resistance to circulating tumor cells. Body weight was consistently reduced by SI across all experiments, similar to previously reported studies in mice and rats, especially in the context of an immune challenge (Andrade et al.,

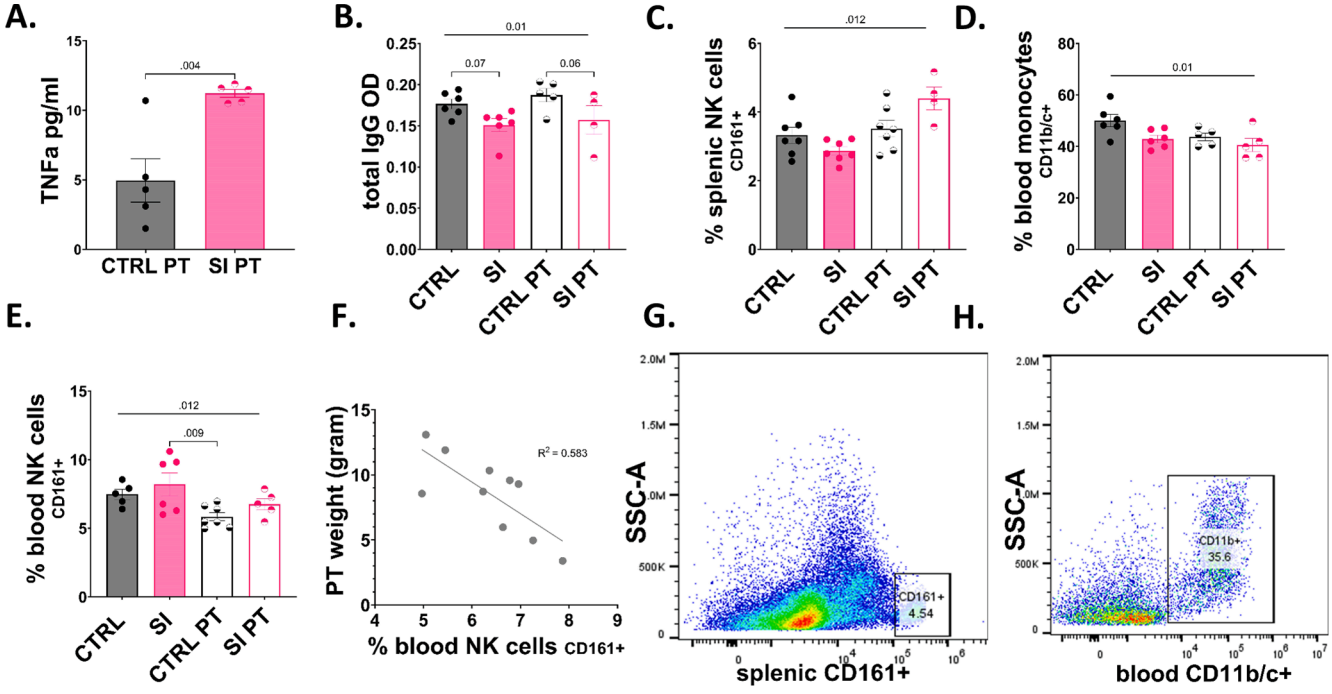

Fig. 7. The effect of long-term SI on TNFα, IgG, and immunocytes in tumor-bearing and naïve rats – Exp 4. (A) TNFα levels (pg/ml). (B) Total IgG optical density values. Flow cytometry analysis: (C) Percentage of CD161 + splenic NK cells. (D) Percentage of CD11b/c + blood cells. (E) Percentage of CD161 + blood NK cells. (G-H) Examples of flow cytometry gating of splenic CD161 and blood CD11b/c + .

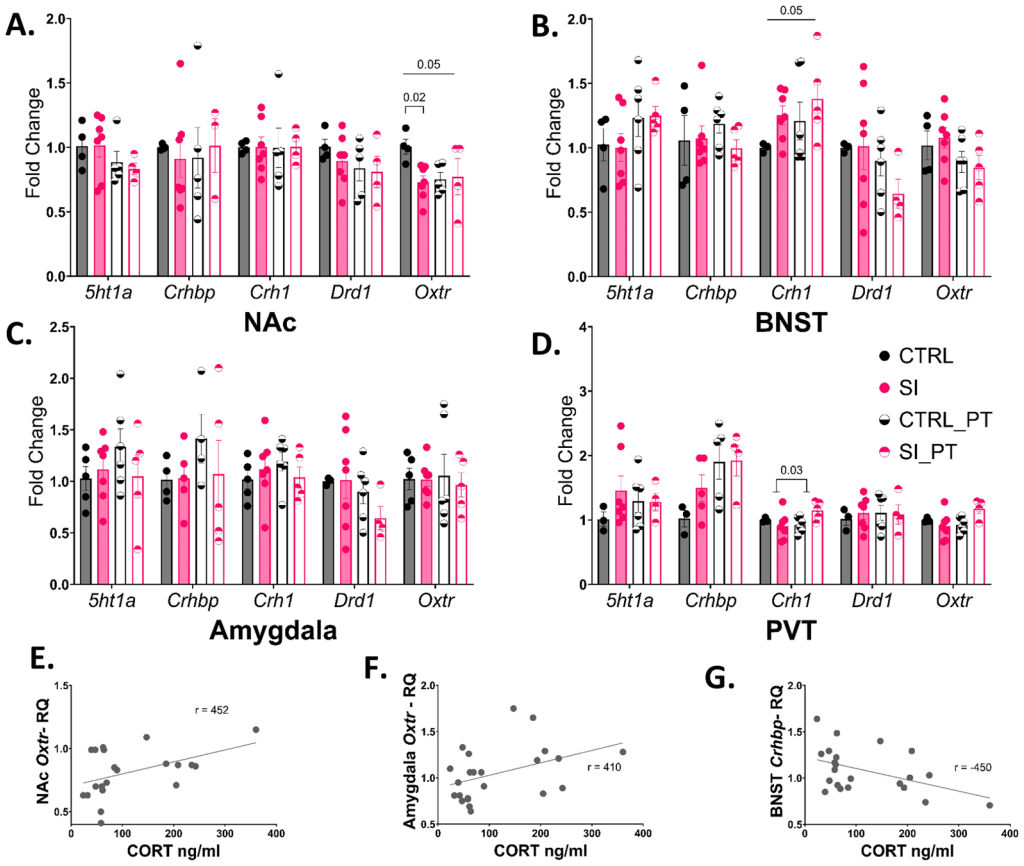

Fig. 8. The effect of long-term SI on gene expression in the NAc, BNST, Amygdala, and the PVT in tumor-bearing and naïve rats – Exp 4. (A) Nucleus accumbens (NAc). (B) Bed nucleus of the stria terminalis (BNST). (C) Amygdala. (D) Paraventricular thalamus (PVT). (E-F) Correlation between *Oxtr* and *Crhbp* gene expression and CORT plasma levels.

2023; Verza et al., 2021). Our work also shows that this decrease in BW is most profound during the first week of SI, and that females BW is affected more than males. Our findings align with previous research and underscore the significant influence of SI on physiological stress responses in rodents (Bledsoe et al., 2011; Borges et al., 2023; Harvey et al., 2019; Hermes et al., 2009).

4.1. *Mixed effects of social isolation on tumor toxicity*

Counterintuitively, SI initiated with PT induction decreased the weight of the developing PTs. Tumor transcriptomic analysis revealed significant tumor molecular alterations: decreased EMT, and decreased transcription activity of NF-kB and CREB. These findings contrast with those from human studies. For example, an increase in EMT and in NF-kB and CREB transcriptional activity was demonstrated in socially isolated cancer patients (Bower et al., 2018; Lutgendorf et al., 2020, 2011). Additionally, while higher levels of social support have been associated with increased TILs and peripheral NK cells in humans (Lutgendorf et al., 2005), the above results indicate that SI (rather than social support) upregulated genes derived from TILs. The discrepancy between this finding and the associations found in cancer patients could be explained by a major generic transcriptional downregulation in PTs from isolated rats. We found a significant number of downregulated genes, and much fewer upregulated genes (4,811 vs. 299, >2-fold difference).

This underscores the profound inhibition of isolation on the tumor transcriptomic activity and of several biological pathways, potentially hindering tumor progression, as may have occurred herein, exhibited by the reduction in weight of PTs subjected to SI. Moreover, SI decreased HIF1a and HIF2a expression, while increasing FOXO3 and FOXO4 TFBMs. These changes are associated with adaptive responses to metabolic stress and may also indicate disruptions in metabolic processes and promotion of cell death (Dai et al., 2020; Farhan et al., 2020). In line with this idea, a recent study found that isolated rats exhibit an increased risk of dormant mammary tumor recurrence after tamoxifen therapy, an effect that was attributed to the suppression of mitochondrial oxidative phosphorylation signaling pathways (Andrade et al., 2023).

4.2. *Thermoregulation as a possible mediating factor*

Unlike humans, who can adapt to temperature changes through clothing, rodents typically rely on close contact with conspecifics to efficiently regulate body temperature, a process which is disrupted by isolation (Ebensperger and Hayes, 2016; Hankenson et al., 2018). The presence of a conspecific to help maintain warmth is particularly crucial in modern laboratory settings, where the ambient temperature is lower than the thermoneutral range for rats, which is above 28 °C (Hankenson et al., 2018; Keller et al., 2022). With the typical vivarium temperature set around 22 °C, which is in itself considered a mild stressor (Hylander et al., 2019), isolation can be particularly detrimental to the rats' thermoregulation. Studies in mice have demonstrated that SI can disrupt metabolic processes by impairing thermoregulation, a phenomenon that can be mitigated by providing an artificial nest (Hamilton et al., 2022; Sun et al., 2014). They also reported that isolated mice significantly reduced weight despite consuming more food, which was reversed when an artificial nest was provided (Hamilton et al., 2022). In our study, we also observed weight loss in isolated rats. Although we did not measure

food intake, it is reasonable to speculate that, to maintain normal body temperature, the isolated rats may have consumed more food, similar to the findings in mice.

These findings suggest additional pathways through which SI can activate the stress system, such as mild hypothermia or cold exposure, which increase HPA and sympathetic nervous system activities, leading to broad changes in body physiology and metabolism (Hu et al., 2022; Ma and Morilak, 2005). Moreover, loneliness and SI have been linked to increased adrenergic activity in humans and primates (Cacioppo et al., 2015; Cole et al., 2021). Thus, in rats, the sympathetic nervous system may also play a significant role in the SI- stress response, impacting immune function. These pathways may play a role in the increased all-cause mortality observed among SI-PT rats compared to CTRL-PT rats, suggesting that compromised metabolism, weight loss, and heightened stress responses contributed to the decreased tumor weight observed in SI rats, while also leading to increased susceptibility to surgery and impaired post-surgery recovery, resulting in higher mortality.

4.3. Sex-specific responses to social isolation

In naïve isolated rats, we measured pro-inflammatory cytokines and total IgG levels. Compared to controls, we observed an increase in IL-6 levels and a decrease in IgG levels in both sexes. Notably, TNFα levels increased in isolated females but decreased in isolated males relative to controls. This sex-specific difference in TNFα levels corresponds with findings from a study in Sprague-Dawley rats, where isolation caused a similar dimorphic effect (Hermes et al., 2006). In this study, female rats bearing tumors exhibited similar patterns of increased TNFα levels and decreased total IgG levels, alongside a reduced percentage of circulating CD11b/c + immunocytes, even three months post- PT excision and following four months of SI. Furthermore, our results parallel a vast body of research on human subjects that shows an increase in IL-6 levels and chronic inflammation in isolated and lonely individuals (Häfner et al., 2011; Matthews et al., 2024; Smith et al., 2020). Moreover, dimorphic sex differences in the characteristics of inflammatory biomarkers were reported by many human studies (Koyama et al., 2021; Qi et al., 2023; Umberson et al., 2022; Yang et al., 2014). The significant negative correlation between IL and 6 and CORT observed in our findings is supported by substantial existing evidence that cortisol and IL-6 are closely linked in a regulatory feedback loop (Pace and Miller, 2009). Therefore, we propose that our results strengthen the understanding of the connection between SI, stress system and its impact on the immune response.

4.4. Neurobiological changes associated with social isolation

In rats, various neurobiological changes have been documented following periods of SI (Fone and Porkess, 2008; Li et al., 2021; Mumtaz et al., 2018). We hypothesized that SI would primarily affect brain regions involved in stress, motivation, and social behavior, and indeed, the NAc, BNST, and PVT exhibited changes in various markers. However, the PVT showed the most pronounced alterations, with reduced *5htr1a*, *Drd1*, and *Oxtr* expression in both sexes, which were highly correlated with changes in other brain regions during both short- and long-term SI. Though understudied in the context of SI, the PVT is a known hub for mediating stress, social, and motivational behaviors (Hsu et al., 2014; Penzo and Gao, 2021; Zhou and Zhu, 2019), integrating threat and arousal signals from the cortex and hypothalamus to regions like the NAc, BNST, and amygdala, which are involved in stress responses and have been documented to be affected by SI (Bendersky et al., 2021; Lavenda-Grosberg et al., 2022; Wang et al., 2012).

In the current study, we examined whether SI impacted the stress pathway—specifically the HPA axis—both centrally and peripherally, by measuring *Crhbp* and *Crh1* expression across four brain regions, and plasma CORT levels. After 5 weeks of SI in females, *Crhbp* expression increased in the PVT and BNST while decreasing in the amygdala. *Crh1* also significantly increased in the BNST and amygdala, with these effects persisting in the BNST after 14 weeks of SI. These central changes in the CRH system during SI are documented in various rodents studies (Bledsoe et al., 2011; Hostetler and Ryabinin, 2013). Additionally, in females, a peripheral effect on the HPA axis was observed after 5 weeks of SI, with increased CORT levels, though no significant effect was seen in males or in females after 14 weeks. CORT level findings in isolated rats have been inconsistent across studies (Alshammari et al., 2020; Harvey et al., 2019; Sladjana and Ljubica, 2005), potentially due to differences in measurement timing and methods. Although we found no significant CORT change after 14 weeks, we observed a significant correlation between *Crhbp* expression in the BNST and plasma CORT levels.

Overall, the increases in *Crhbp* and *Crh1* expression in brain regions, along with the peripheral increase in CORT and the significant central-peripheral correlations, suggest that SI activates both central and peripheral stress responses, acting as a chronic stressor. This suggests that the HPA axis may be a primary pathway through which SI impacts peripheral immunity, aligning with growing evidence linking chronic stress to immune dysregulation and heightened inflammatory responses (Chu et al., 2024; Hermes et al., 2006).

We examined the impact of SI on oxytocin, which is involved in social bonding, social behavior, and stress regulation through the CRH system (Winter and Jurek, 2019). SI had both short and long-lasting effects on *Oxtr* expression in the NAc and the PVT. Our findings align with substantial evidence linking oxytocin to SI, both centrally and peripherally (Grippo et al., 2009; Oliveira et al., 2019). For instance, in aged F344 rats, *Oxtr* expression were elevated in the BNST (Perkins et al., 2019). Moreover, *Oxtr* expression in the PVT was highly correlated with *Crhbp* and *Crh1* in other regions across animals. We also observed a significant positive correlation between plasma CORT levels and *Oxtr* expression in the NAc and amygdala following 14 weeks of SI in females. These findings support the well-established connection between CRH and oxytocin signaling pathways, which play a key role in stress regulation (Hostetler and Ryabinin, 2013; Winter and Jurek, 2019). The downregulation of *Oxtr* in the PVT and NAc suggests altered oxytocin signaling, potentially leading to increased stress responses through the CRH-oxytocin system, altered social behaviors, and direct impacts on the immune system (Haykin and Rolls, 2021; Schiller et al., 2021).

The serotonergic and dopaminergic systems were also hypothesized to be affected by SI, as they are known to play key roles in social behavior, learning, motivation, and affiliation (Frey and McCabe, 2020; Schmidt et al., 2020). Indeed, we report changes to *DRD1,* particularly in males*, and 5htra1* upregulation in the PVT and the amygdala in both sexes, but only in the BNST in females. Our results align with other studies linking SI and altered serotonin and dopamine signaling (Ago et al., 2014; da Silva et al., 2024; Mumtaz et al., 2018; Vitale and Smith, 2022), and suggest that SI can lead to reduced activation of the reward and motivation pathway, as social interactions are a primary source of natural rewards (Krach et al., 2010). Moreover, these alterations in serotonergic signaling could manifest as increased anxiety or depressive-like behaviors, and potentially lead to anhedonia, which are common outcomes of SI in both humans and rodents (Grippo et al., 2007; Liu et al., 2019; Tan et al., 2020). Although there is some evidence that dopamine and serotonergic signaling interact with the peripheral immune system (Haykin and Rolls, 2021), the exact mechanisms remain largely unknown.

Fundamental sex differences have been reported in stress response and social behavior in rats (Barnard et al., 2019; Howerton et al., 2014), and our findings reflect these dimorphisms. Specifically, females exhibited significant alterations in the stress pathway and a reduction in BW, while males showed a decrease in TNFα and more pronounced changes in *Drd1*. These align with numerous studies highlighting sex differences in responses to SI (Kinley et al., 2021; Oliveira et al., 2019), such as increased vigilance to stressors in females (Weintraub et al., 2010) and decreased sociability coupled with increased aggression in

males (Perkins et al., 2019). These observations suggest that SI affects both sexes but likely through distinct mechanisms, particularly concerning behavioral phenotypes.

In sum, the underlying mechanisms through which SI impacts the peripheral immune system likely involve complex interactions between the HPA axis and the oxytocin, dopaminergic, and serotonergic systems, which are known to be closely interlinked (Winter and Jurek, 2019). Future studies focusing on the effects of SI on CNS mechanisms and their downstream impacts on immunity are warranted.

4.5. Limitations and future directions

Our study provides significant insights into the effects of SI on both naïve and tumor-bearing rats. However, there are several limitations to consider. The use of the MADB106 tumor cell line, which does not metastasize spontaneously, may not be an ideal model to study cancer mortality. Additionally, there are limited immunological assays available for rats compared to mice, from sensitive ELISA kits to various flow cytometry antibodies. Although rats are highly social and suited for social-behavioral studies, the lack of diverse immunological tools constrains our understanding of the link between SI and the immune system.

Our study provides a comprehensive approach by showing both central and peripheral effects of SI on naïve and cancer-bearing rats. While our results provide a broad and solid foundation for identifying possible neuro-immune targets, the mechanistic insights remain limited. Intervention studies are necessary to identify the exact mechanisms, likely involving several pathways, by which SI impacts immunity, such as increasing metastases. For example, pharmacological interventions should be explored, such as beta-blockers and COX-2 inhibitors, which have been found to reduce metastases by modulating adrenergic signaling and reducing inflammation (Sorski et al., 2016). Another pharmacological approach could involve administering oxytocin agonists and measuring their impact on peripheral immunity. This would offer further insights into the role of oxytocin in the context of SI and its effects on immunity. Moreover, the mechanisms by which SI may affect rats could differ from those in humans, primarily because rats rely on conspecifics for social thermoregulation, making some results non-translatable to humans. Despite these differences, there are multiple parallels between humans and rats in the effects of SI, such as its impact on social interaction and reward, and the activation of the HPA axis (Gądek-Michalska et al., 2017; Pisu et al., 2016).

Our prolonged SI experiment (14 weeks) was conducted only in females, due to the use of implantable mammary tumor, and our initial findings indicated that females were substantially more impacted than males. The longer-term effects of SI on males remain to be studied. While we did not assess the estrus cycle of female rats, which may have influenced the results (Ben-Eliyahu et al., 2000), the inclusion of both sexes and the use of control groups likely mitigated this potential variability. Moreover, similar variability was observed in both sexes in both the SI and CTRL groups. Future studies should consider monitoring the estrus cycle to fully understand its impact on the observed SI effects.

Finally, in this study, the changes in brain and tumor transcriptome were assessed only at the mRNA level and not at the protein level. This limits our understanding of the physiological functions, as changes in mRNA expression do not always correlate directly with protein expression. However, mRNA data remain highly valuable as they provide key insights into gene expression changes and the molecular pathways impacted by SI, and they are widely used in similar studies to understand early molecular events influenced by behavioral changes (Begni et al., 2020; Borges et al., 2023; Wang et al., 2017). These findings serve as a crucial foundation for future studies, which should include protein-level assessments to provide a more comprehensive understanding of the mechanisms behind the impact of SI.

5. Conclusion

Our study provides further evidence of the detrimental effects of SI on immunity, metastasis progression, and rat welfare. It also hints at novel neurobiological-immune mechanisms, which may underlie SI effects, suggesting that the PVT may be a key region involved in affecting various neural systems such as the HPA axis, *OXTR*, *Drd1*, and *5htr1a* within the NAc, BNST, and amygdala. We demonstrate, for the first time, that SI can increase the number of metastases in rats, and, similar to other studies, elevates pro-inflammatory cytokines and mortality. Additionally, our findings indicate that SI exerts a long-lasting and profound effect on peripheral immunity and body physiology, potentially impacting the body's ability to maintain homeostasis. Notably, the impact of SI on thermoregulation is another critical factor, as the lack of social thermoregulation may exacerbate the physiological stress experienced by isolated rats, further compromising their health. We urge researchers to avoid single-housing in experiments when possible, as this practice can significantly contribute to physiological stress and skew results. Our causal results align with a vast body of pioneering correlative evidence showing that SI and perceived loneliness in humans are associated with increased inflammation and malignancies, poorer health, and higher mortality (Cacioppo et al., 2015; Steptoe et al., 2013). SI alone can negatively affect various physiological systems, and immune and/or medical challenges like cancer may act as a double-hit stressor (Sailer et al., 2022; Shangase et al., 2022). Further investigation into the mechanisms of SI using targeted interventions, such as pharmacological or thermoregulatory manipulations, is necessary to unveil the underlying mechanisms and mitigate these harmful effects. This work underscores the importance of considering social needs when treating cancer patients, as a supportive social environment may enhance physical recovery, well-being, and resistance to post-operative metastasis.

CRediT authorship contribution statement

Estherina Trachtenberg: Writing – original draft, Visualization, Methodology, Formal analysis, Data curation, Conceptualization. **Keren Ruzal:** Writing – review & editing, Data curation. **Elad Sandbank:** Writing – review & editing, Data curation. **Einat Bigelman:** Methodology, Data curation. **Itay Ricon-Becker:** Writing – review & editing, Methodology. **Steve W. Cole:** Writing – review & editing, Supervision, Resources, Methodology, Data curation. **Shamgar Ben-Eliyahu:** Writing – review & editing, Supervision, Resources, Conceptualization. **Inbal Ben-Ami Bartal:** Writing – review & editing, Supervision, Resources, Methodology, Funding acquisition.

Declaration of Competing Interest

The authors declare that they have no known competing financial interests or personal relationships that could have appeared to influence the work reported in this paper.

Data availability

Data will be made available on request.

Acknowledgements

The authors would like to express their gratitude to Ella Rosen, Bar Shvalbo, and Noam Ben-Shalom for their invaluable help and advice. We also extend our thanks to the Azrieli Foundation, the Israel Science Foundation, and the Milner Foundation for their generous funding of our research.

Appendix A. Supplementary data

Supplementary data to this article can be found online at https://doi.org/10.1016/j.bbi.2024.10.005.

References

Ago, Y., Takuma, K., Matsuda, T., 2014. The potential role of serotonin1a receptors in post-weaning social isolation-induced abnormal behaviors in rodents. J. Pharmacol. Sci. 125, 237–241. https://doi.org/10.1254/jphs.14R05CP.

Alshammari, A., Alduhailan, H., Saja, M., Alrasheed, N., Alshammari, M., 2020. Examining the central effects of chronic stressful social isolation on rats. Biomed. Rep. 13, 1. https://doi.org/10.3892/br.2020.1363.

Barnard, D.F., Gabella, K.M., Kulp, A.C., Parker, A.D., Dugan, P.B., Johnson, J.D., 2019. Sex differences in the regulation of brain IL-1β in response to chronic stress. Psychoneuroendocrinology 103, 203–211. https://doi.org/10.1016/j.psyneuen.2019.01.026.

Begni, V., Sanson, A., Pfeiffer, N., Brandwein, C., Inta, D., Talbot, S.R., Riva, M.A., Gass, P., Mallien, A.S., 2020. Social isolation in rats: effects on animal welfare and molecular markers for neuroplasticity. PLOS ONE 15, e0240439.

Bendersky, C.J., Milian, A.A., Andrus, M.D., De La Torre, U., Walker, D.M., 2021. Long-term impacts of post-weaning social isolation on nucleus accumbens function. Front. Psychiatry 12. https://doi.org/10.3389/fpsyt.2021.745406.

Ben-Eliyahu, S., Shakhar, G., Shakhar, K., Melamed, R., 2000. Timing within the oestrous cycle modulates adrenergic suppression of NK activity and resistance to metastasis: possible clinical implications. Br. J. Cancer 83, 1747–1754. https://doi.org/10.1054/bjoc.2000.1563.

Ben-Shaanan, T.L., Azulay-Debby, H., Dubovik, T., Starosvetsky, E., Korin, B., Schiller, M., Green, N.L., Admon, Y., Hakim, F., Shen-Orr, S.S., Rolls, A., 2016. Activation of the reward system boosts innate and adaptive immunity. Nat. Med. 22, 940–944. https://doi.org/10.1038/nm.4133.

Bledsoe, A.C., Oliver, K.M., Scholl, J.L., Forster, G.L., 2011. Anxiety states induced by post-weaning social isolation are mediated by CRF receptors in the dorsal raphe nucleus. Brain Res. Bull. 85, 117–122. https://doi.org/10.1016/j.brainresbull.2011.03.003.

Borges, J.V., Pires, V.N., de Freitas, B.S., Rübensam, G., de Vieira, V.C., Souza dos Santos, C., Schröder, N., Bromberg, E., 2023. Behavior, BDNF and epigenetic mechanisms in response to social isolation and social support in middle aged rats exposed to chronic stress. Behav. Brain Res. 441, 114303. https://doi.org/10.1016/j.bbr.2023.114303.

Bower, J.E., Shiao, S.L., Sullivan, P., Lamkin, D.M., Atienza, R., Mercado, F., Arevalo, J., Asher, A., Ganz, P.A., Cole, S.W., 2018. Prometastatic molecular profiles in breast tumors from socially isolated women. JNCI Cancer Spectr. 2, pky029. https://doi.org/10.1093/jncics/pky029.

Bromberg-Martin, E.S., Matsumoto, M., Hikosaka, O., 2010. Dopamine in motivational control: rewarding, aversive, and alerting. Neuron 68, 815–834. https://doi.org/10.1016/j.neuron.2010.11.022.

Cacioppo, C.S., Capitanio, J.P., Cole, S.W., 2015. The neuroendocrinology of social isolation. Annu. Rev. Psychol. 66, 733–767. https://doi.org/10.1146/annurev-psych-010814-015240.

Cacioppo, J., Hawkley, L., Thisted, R., 2010. Perceived social isolation makes me sad. Psychol. Aging 25, 453–463. https://doi.org/10.1037/a0017216.Perceived.

Carter, C.S., Kenkel, W.M., MacLean, E.L., Wilson, S.R., Perkeybile, A.M., Yee, J.R., Ferris, C.F., Nazarloo, H.P., Porges, S.W., Davis, J.M., Connelly, J.J., Kingsbury, M. A., 2020. Is oxytocin "nature's medicine"? Pharmacol. Rev. 72, 829–861. https://doi.org/10.1124/pr.120.019398.

Choi, Y.-L., Bocanegra, M., Kwon, M.J., Shin, Y.K., Nam, S.J., Yang, J.-H., Kao, J., Godwin, A.K., Pollack, J.R., 2010. LYN is a mediator of epithelial-mesenchymal transition and target of dasatinib in breast cancer. Cancer Res. 70, 2296. https://doi.org/10.1158/0008-5472.CAN-09-3141.

Chu, B., Marwaha, K., Sanvictores, T., Awosika, A.O., Ayers, D., 2024. Physiology, Stress Reaction, in: StatPearls. StatPearls Publishing, Treasure Island (FL).

Cole, S.W., Yan, W., Galic, Z., Arevalo, J., Zack, J.A., 2005. Expression-based monitoring of transcription factor activity: the TELiS database. Bioinformatics 21, 803–810. https://doi.org/10.1093/bioinformatics/bti038.

Cole, S.W., Cacioppo, J.T., Cacioppo, S., Bone, K., Del Rosso, L.A., Spinner, A., Arevalo, J. M.G., Dizon, T.P., Capitanio, J.P., 2021. The Type I interferon antiviral gene program is impaired by lockdown and preserved by caregiving. Proc. Natl. Acad. Sci. 118. https://doi.org/10.1073/pnas.2105803118 e2105803118.

Conrad, K.L., Louderback, K.M., Gessner, C.P., Winder, D.G., 2011. Stress-induced alterations in anxiety-like behavior and adaptations in plasticity in the bed nucleus of the stria terminalis. Physiol. Behav., 2010 Neurobiology of Stress Workshop 104, 248–256. https://doi.org/10.1016/j.physbeh.2011.03.001.

Corsi-Zuelli, F., Fachim, H.A., Loureiro, C.M., Shuhama, R., Bertozi, G., Joca, S.R.L., Menezes, P.R., Louzada-Junior, P., Del-Ben, C.M., 2019. Prolonged periods of social isolation from weaning reduce the anti-inflammatory cytokine IL-10 in blood and brain. Front. Neurosci. 12. https://doi.org/10.3389/fnins.2018.01011.

da Silva, R.P.B., Pinheiro, I.L., da Silva, R.K.B., Moretti, E.C., de Oliveira Neto, O.B., Ferraz-Pereira, K., Galindo, L.C.M., 2024. Social isolation and post-weaning environmental enrichment effects on rat emotional behavior and serotonergic system. Int. J. Dev. Neurosci. Off. J. Int. Soc. Dev. Neurosci. https://doi.org/10.1002/jdn.10324.

Dai, C., Chen, X., Li, J., Comish, P., Kang, R., Tang, D., 2020. Transcription factors in ferroptotic cell death. Cancer Gene Ther. 27, 645–656. https://doi.org/10.1038/s41417-020-0170-2.

Dawes, R.P., Burke, K.A., Byun, D.K., Xu, Z., Stastka, P., Chan, L., Brown, E.B., Madden, K.S., 2020. Chronic stress exposure suppresses mammary tumor growth and reduces circulating exosome TGF-β content via β-adrenergic receptor signaling in MMTV-PyMT Mice. Breast Cancer Basic Clin. Res. 14, 18–21. https://doi.org/10.1177/1178223420931511.

Dayer, A., 2014. Serotonin-related pathways and developmental plasticity: relevance for psychiatric disorders. Dialogues Clin. Neurosci. 16, 29. https://doi.org/10.31887/DCNS.2014.16.1/adayer.

de Andrade, F.O., Jin, L., Clarke, R., Wood, I., Dutton, M., Anjorin, C., Rubin, G., Gao, A., Sengupta, S., FitzGerald, K., Hilakivi-Clarke, L., 2023. Social isolation activates dormant mammary tumors, and modifies inflammatory and mitochondrial metabolic pathways in the rat mammary gland. Cells 12, 961. https://doi.org/10.3390/cells12060961.

de Boer, S.F., Koolhaas, J.M., 2024. The laboratory rat, in: The UFAW Handbook on the Care and Management of Laboratory and Other Research Animals. John Wiley & Sons, Ltd, pp. 379–399. https://doi.org/10.1002/9781119555278.ch22.

De la Roca-Chiapas, J.M., Barbosa-Sabanero, G., Martínez-García, J.A., Martínez-Soto, J., González-Ramírez, L.P., Ramos Frausto, V.M., Nowack, K., 2016. Impact of stress and levels of corticosterone on the development of breast cancer in rats. Psychol. Res. Behav. Manage. 1. https://doi.org/10.2147/PRBM.S94177.

de Oliveira, V.E.M., Neumann, I.D., de Jong, T.R., 2019. Post-weaning social isolation exacerbates aggression in both sexes and affects the vasopressin and oxytocin system in a sex-specific manner. Neuropharmacology 156, 107504. https://doi.org/10.1016/j.neuropharm.2019.01.019.

Dolen, G., Darvishzadeh, A., Huang, K.W., Malenka, R.C., 2013. Social reward requires coordinated activity of nucleus accumbens oxytocin and serotonin. Nature 501, 179–184. https://doi.org/10.1038/nature12518.

Du Preez, A., Law, T., Onorato, D., Lim, Y.M., Eiben, P., Musaelyan, K., Egeland, M., Hye, A., Zunszain, P.A., Thuret, S., Pariante, C.M., Fernandes, C., 2020. The type of stress matters: repeated injection and permanent social isolation stress in male mice have a differential effect on anxiety- and depressive-like behaviours, and associated biological alterations. Transl. Psychiatry 10, 325. https://doi.org/10.1038/s41398-020-01000-3.

Dunphy-Doherty, F., O'Mahony, S.M., Peterson, V.L., O'Sullivan, O., Crispie, F., Cotter, P.D., Wigmore, P., King, M.V., Cryan, J.F., Fone, K.C.F., 2018. Post-weaning social isolation of rats leads to long-term disruption of the gut microbiota-immune-brain axis. Brain. Behav. Immun. 68, 261–273. https://doi.org/10.1016/j.bbi.2017.10.024.

Ebensperger, L.A., Hayes, L.D., 2016. Causes and evolution of group-living, in: Sociobiology of Caviomorph Rodents. John Wiley & Sons, Ltd, pp. 173–200. https://doi.org/10.1002/9781118846506.ch7.

Farhan, M., Silva, M., Xingan, X., Huang, Y., Zheng, W., 2020. Role of FOXO transcription factors in cancer metabolism and angiogenesis. Cells 9, 1586. https://doi.org/10.3390/cells9071586.

Fone, K.C.F., Porkess, M.V., 2008. Behavioural and neurochemical effects of post-weaning social isolation in rodents—Relevance to developmental neuropsychiatric disorders. Neurosci. Biobehav. Rev 32, 1087–1102. https://doi.org/10.1016/j.neubiorev.2008.03.003.

Frey, A.-L., McCabe, C., 2020. Effects of serotonin and dopamine depletion on neural prediction computations during social learning. Neuropsychopharmacology 45, 1431–1437. https://doi.org/10.1038/s41386-020-0678-z.

Gądek-Michalska, A., Bugajski, A., Tadeusz, J., Rachwalska, P., Bugajski, J., 2017. Chronic social isolation in adaptation of HPA axis to heterotypic stress. Pharmacol. Rep. 69, 1213–1223. https://doi.org/10.1016/j.pharep.2017.08.011.

Garcia-Garcia, A., Tancredi, A.N., Leonardo, E.D., 2014. 5-HT1A receptors in mood and anxiety: recent insights into autoreceptor versus heteroreceptor function. Psychopharmacology (berl.) 231, 623–636. https://doi.org/10.1007/s00213-013-3389-x.

Grippo, A.J., Cushing, B.S., Carter, C.S., 2007. Depression-like behavior and stressor-induced neuroendocrine activation in female prairie voles exposed to chronic social isolation. Psychosom. Med. 69, 149. https://doi.org/10.1097/PSY.0b013e31802f054b.

Grippo, A.J., Trahanas, D.M., Zimmerman, R.R., Porges, S.W., Carter, C.S., 2009. Oxytocin protects against negative behavioral and autonomic consequences of long-term social isolation. Psychoneuroendocrinology 34, 1542–1553. https://doi.org/10.1016/j.psyneuen.2009.05.017.

Häfner, S., Emeny, R.T., Lacruz, M.E., Baumert, J., Herder, C., Koenig, W., Thorand, B., Ladwig, K.H., 2011. Association between social isolation and inflammatory markers in depressed and non-depressed individuals: results from the MONICA/KORA study. Brain. Behav. Immun. 25, 1701–1707. https://doi.org/10.1016/j.bbi.2011.06.017.

Haldar, R., Berger, L.S., Rossenne, E., Radin, A., Eckerling, A., Sandbank, E., Sloan, E.K., Cole, S.W., Ben-Eliyahu, S., 2023. Perioperative escape from dormancy of spontaneous micro-metastases: a role for malignant secretion of IL-6, IL-8, and VEGF, through adrenergic and prostaglandin signaling. Brain. Behav. Immun. 109, 175–187. https://doi.org/10.1016/j.bbi.2023.01.005.

Hamilton, A., Rizzo, R., Brod, S., Ono, M., Perretti, M., Cooper, D., D'Acquisto, F., 2022. The immunomodulatory effects of social isolation in mice are linked to temperature control. Brain. Behav. Immun. 102, 179–194. https://doi.org/10.1016/j.bbi.2022.02.022.

Hankenson, F.C., Marx, J.O., Gordon, C.J., David, J.M., 2018. Effects of rodent thermoregulation on animal models in the research environment. Comp. Med. 68, 425–438. https://doi.org/10.30802/AALAS-CM-18-000049.

Harvey, B.H., Regenass, W., Dreyer, W., Möller, M., 2019. Social isolation rearing-induced anxiety and response to agomelatine in male and female rats: Role of corticosterone, oxytocin, and vasopressin. J. Psychopharmacol. (oxf.) 33, 640–646. https://doi.org/10.1177/0269881119826783.

Haykin, H., Rolls, A., 2021. The neuroimmune response during stress: a physiological perspective. Immunity 54, 1933–1947. https://doi.org/10.1016/j.immuni.2021.08.023.

Herman, J.P., McKlveen, J.M., Ghosal, S., Kopp, B., Wulsin, A., Makinson, R., Scheimann, J., Myers, B., 2016. Regulation of the hypothalamic-pituitary-adrenocortical stress response. Compr. Physiol. 6, 603–621. https://doi.org/10.1002/cphy.c150015.

Hermes, G.L., Delgado, B., Tretiakova, M., Cavigelli, S.A., Krausz, T., Conzen, S.D., McClintock, M.K., 2009. Social isolation dysregulates endocrine and behavioral stress while increasing malignant burden of spontaneous mammary tumors. Proc. Natl. Acad. Sci. u. s. a. 106, 22393–22398. https://doi.org/10.1073/pnas.0910753106.

Hermes, G.L., McClintock, M.K., 2008. Isolation and the timing of mammary gland development, gonadarche, and ovarian senescence: Implications for mammary tumor burden. Dev. Psychobiol. 50, 353–360. https://doi.org/10.1002/dev.20295.

Hermes, G.L., Rosenthal, L., Montag, A., McClintock, M.K., 2006. Social isolation and the inflammatory response: sex differences in the enduring effects of a prior stressor. Am. J. Physiol. Regul. Integr. Comp. Physiol. 290, R273–R282. https://doi.org/10.1152/ajpregu.00368.2005.

Holt-Lunstad, J., Smith, T.B., Baker, M., Harris, T., Stephenson, D., 2015. Loneliness and social isolation as risk factors for mortality: a meta-analytic review. Perspect. Psychol. Sci. 10, 227–237. https://doi.org/10.1177/1745691614568352.

Hostetler, C.M., Ryabinin, A.E., 2013. The CRF system and social behavior: a review. Front. Neurosci. 7, 92. https://doi.org/10.3389/fnins.2013.00092.

Howerton, A.R., Roland, A.V., Fluharty, J.M., Marshall, A., Chen, A., Daniels, D., Beck, S. G., Bale, T.L., 2014. Sex differences in corticotropin-releasing factor receptor-1 action within the dorsal raphe nucleus in stress responsivity. Biol. Psychiatry 75, 873–883. https://doi.org/10.1016/j.biopsych.2013.10.013.

Hsu, D.T., Kirouac, G.J., Zubieta, J.-K., Bhatnagar, S., 2014. Contributions of the paraventricular thalamic nucleus in the regulation of stress, motivation, and mood. Front. Behav. Neurosci. 8. https://doi.org/10.3389/fnbeh.2014.00073.

Hu, Y., Liu, Y., Li, S., 2022. Effect of acute cold stress on neuroethology in mice and establishment of its model. Animals 12, 2671. https://doi.org/10.3390/ani12192671.

Hylander, B.L., Gordon, C.J., Repasky, E.A., 2019. Manipulation of ambient housing temperature to study the impact of chronic stress on immunity and cancer in mice. J. Immunol. Baltim. Md 1950 (202), 631–636. https://doi.org/10.4049/jimmunol.1800621.

Iglesias, A.G., Flagel, S.B., 2021. The paraventricular thalamus as a critical node of motivated behavior via the hypothalamic-thalamic-striatal circuit. Front. Integr. Neurosci. 15. https://doi.org/10.3389/fnint.2021.706713.

Jiang, J., Yang, M., Tian, M., Chen, Z., Xiao, L., Gong, Y., 2023. Intertwined associations between oxytocin, immune system and major depressive disorder. Biomed. Pharmacother. 163, 114852. https://doi.org/10.1016/j.biopha.2023.114852.

Kalin, N.H., 2018. Corticotropin-releasing hormone binding protein (CRHBP): stress, psychopathology, and antidepressant treatment response. Am. J. Psychiatry 175, 204–206. https://doi.org/10.1176/appi.ajp.2018.18010059.

Keller, A.C., Chun, J.H., Knaub, L.A., Henckel, M.M., Hull, S.E., Scalzo, R.L., Pott, G.B., Walker, L.A., Reusch, J.E.B., 2022. Thermoneutrality induces vascular dysfunction and impaired metabolic function in male Wistar rats: a new model of vascular disease. J. Hypertens. 40, 2133. https://doi.org/10.1097/HJH.0000000000003153.

Kinley, B.L., Kyne, Robert, F., Lawton-Stone, T.S., Walker, D.M., Paul, M.J., 2021. Long-term consequences of peri-adolescent social isolation on social preference, anxiety-like behavior, and vasopressin neural circuitry of male and female rats. Eur. J. Neurosci. 54, 7790–7804. https://doi.org/10.1111/ejn.15520.

Koyama, Y., Nawa, N., Yamaoka, Y., Nishimura, H., Sonoda, S., Kuramochi, J., Miyazaki, Y., Fujiwara, T., 2021. Interplay between social isolation and loneliness and chronic systemic inflammation during the COVID-19 pandemic in Japan: Results from U-CORONA study. Brain. Behav. Immun. 94, 51–59. https://doi.org/10.1016/j.bbi.2021.03.007.

Krach, S., Paulus, F.M., Bodden, M., Kircher, T., 2010. The rewarding nature of social interactions. Front. Behav. Neurosci. 4. https://doi.org/10.3389/fnbeh.2010.00022.

Lavenda-Grosberg, D., Lalzar, M., Leser, N., Yaseen, A., Malik, A., Maroun, M., Barki-Harrington, L., Wagner, S., 2022. Acute social isolation and regrouping cause short- and long-term molecular changes in the rat medial amygdala. Mol. Psychiatry 27, 886–895. https://doi.org/10.1038/s41380-021-01342-4.

Li, Y., Chen, Z., Zhao, J., Yu, H., Chen, X., He, Y., Tian, Y., Wang, Y., Chen, C., Cheng, K., Xie, P., 2022. Neurotransmitter and related metabolic profiling in the nucleus accumbens of chronic unpredictable mild stress-induced anhedonia-like rats. Front. Behav. Neurosci. 16, 862683. https://doi.org/10.3389/fnbeh.2022.862683.

Li, D.C., Hinton, E.A., Gourley, S.L., 2021. Persistent behavioral and neurobiological consequences of social isolation during adolescence. Semin. Cell Dev. Biol., Special issue: Cortical Development edited by Helen Cooper and Cecilia Flores / Special issue: Heart generation and regeneration edited by Chulan Kwon and Emmanouil Tampakakis 118, 73–82. https://doi.org/10.1016/j.semcdb.2021.05.017.

Liu, N., Wang, Y., An, A.Y., Banker, C., Qian, Y.H., O'Donnell, J.M., 2019. Single housing-induced effects on cognitive impairment and depression-like behavior in male and female mice involve neuroplasticity-related signaling. Eur. J. Neurosci. 1–11. https://doi.org/10.1111/ejn.14565.

Lutgendorf, S.K., Sood, A.K., Anderson, B., McGinn, S., Maiseri, H., Dao, M., Sorosky, J.I., De Geest, K., Ritchie, J., Lubaroff, D.M., 2005. Social Support, psychological distress, and natural killer cell activity in ovarian cancer. J. Clin. Oncol. 23, 7105–7113. https://doi.org/10.1200/JCO.2005.10.015.

Lutgendorf, S.K., DeGeest, K., Dahmoush, L., Farley, D., Penedo, F., Bender, D., Goodheart, M., Buekers, T.E., Mendez, L., Krueger, G., 2011. Social isolation is associated with elevated tumor norepinephrine in ovarian carcinoma patients. Brain. Behav. Immun. 25, 250–255. https://doi.org/10.1016/j.bbi.2010.10.012.

Lutgendorf, S.K., Thaker, P.H., Arevalo, J.M., Goodheart, M.J., Slavich, G.M., Sood, A.K., Cole, S.W., 2018. Biobehavioral modulation of the exosome transcriptome in ovarian carcinoma. Cancer 124, 580–586. https://doi.org/10.1002/cncr.31078.

Lutgendorf, S.K., Penedo, F., Goodheart, M.J., Dahmoush, L., Arevalo, J.M.G., Thaker, P. H., Slavich, G.M., Sood, A.K., Cole, S.W., 2020. Epithelial-mesenchymal transition polarization in ovarian carcinomas from patients with high social isolation. Cancer 126, 4407–4413. https://doi.org/10.1002/cncr.33060.

Ma, S., Morilak, D.A., 2005. Chronic intermittent cold stress sensitises the hypothalamic-pituitary-adrenal response to a novel acute stress by enhancing noradrenergic influence in the rat paraventricular nucleus. J. Neuroendocrinol. 17, 761–769. https://doi.org/10.1111/j.1365-2826.2005.01372.x.

Madden, K.S., Szpunar, M.J., Brown, E.B., 2013. Early impact of social isolation and breast tumor progression in mice. Brain. Behav. Immun. 30, S135–S141. https://doi.org/10.1016/j.bbi.2012.05.003.

Martinez, F.O., Gordon, S., Locati, M., Mantovani, A., 2006. Transcriptional profiling of the human monocyte-to-macrophage differentiation and polarization: new molecules and patterns of gene expression1. J. Immunol. 177, 7303–7311. https://doi.org/10.4049/jimmunol.177.10.7303.

Matthews, T., Rasmussen, L.J.H., Ambler, A., Danese, A., Eugen-Olsen, J., Fancourt, D., Fisher, H.L., Iversen, K.K., Schultz, M., Sugden, K., Williams, B., Caspi, A., Moffitt, T. E., 2024. Social isolation, loneliness, and inflammation: a multi-cohort investigation in early and mid-adulthood. Brain. Behav. Immun. 115, 727–736. https://doi.org/10.1016/j.bbi.2023.11.022.

Mehdi, S.F., Pusapati, S., Khenhrani, R.R., Farooqi, M.S., Sarwar, S., Alnasarat, A., Mathur, N., Metz, C.N., LeRoith, D., Tracey, K.J., Yang, H., Brownstein, M.J., Roth, J., 2022. Oxytocin and related peptide hormones: candidate anti-inflammatory therapy in early stages of sepsis. Front. Immunol. 13. https://doi.org/10.3389/fimmu.2022.864007.

Möller, M., Du Preez, J.L., Viljoen, F.P., Berk, M., Emsley, R., Harvey, B.H., 2013. Social isolation rearing induces mitochondrial, immunological, neurochemical and behavioural deficits in rats, and is reversed by clozapine or N-acetyl cysteine. Brain. Behav. Immun. 30, 156–167. https://doi.org/10.1016/j.bbi.2012.12.011.

Mumtaz, F., Khan, M.I., Zubair, M., Dehpour, A.R., 2018. Neurobiology and consequences of social isolation stress in animal model—A comprehensive review. Biomed. Pharmacother. 105, 1205–1222. https://doi.org/10.1016/j.biopha.2018.05.086.

Pace, T.W.W., Miller, A.H., 2009. Cytokines and Glucocorticoid receptor signaling: relevance to major depression. Ann. n. y. Acad. Sci. 1179, 86. https://doi.org/10.1111/j.1749-6632.2009.04984.x.

Panossian, A., Cave, M.W., Patel, B.A., Brooks, E.L., Flint, M.S., Yeoman, M.S., 2020. Effects of age and social isolation on murine hippocampal biochemistry and behavior. Mech. Ageing Dev. 191, 111337. https://doi.org/10.1016/j.mad.2020.111337.

Penzo, M.A., Gao, C., 2021. The paraventricular nucleus of the thalamus: an integrative node underlying homeostatic behavior. Trends Neurosci. 44, 538–549. https://doi.org/10.1016/j.tins.2021.03.001.

Perkins, A.E., Varlinskaya, E.I., Deak, T., 2019. Impact of housing conditions on social behavior, neuroimmune markers, and oxytocin receptor expression in aged male and female Fischer 344 rats. Exp. Gerontol. 123, 24–33. https://doi.org/10.1016/j.exger.2019.05.005.

Pisu, M.G., Garau, A., Boero, G., Biggio, F., Pibiri, V., Dore, R., Locci, V., Paci, E., Porcu, P., Serra, M., 2016. Sex differences in the outcome of juvenile social isolation on HPA axis function in rats. Neuroscience 320, 172–182. https://doi.org/10.1016/j.neuroscience.2016.02.009.

Powell, N.D., Sloan, E.K., Bailey, M.T., Arevalo, J.M.G., Miller, G.E., Chen, E., Kobor, M. S., Reader, B.F., Sheridan, J.F., Cole, S.W., 2013. Social stress up-regulates inflammatory gene expression in the leukocyte transcriptome via β-adrenergic induction of myelopoiesis. Proc. Natl. Acad. Sci. u. s. a. 110, 16574–16579. https://doi.org/10.1073/pnas.1310655110.

Qi, X., Ng, T.K.S., Wu, B., 2023. Sex differences in the mediating role of chronic inflammation on the association between social isolation and cognitive functioning among older adults in the United States. Psychoneuroendocrinology 149, 106023. https://doi.org/10.1016/j.psyneuen.2023.106023.

Sailer, L.L., Patel, P.P., Park, A.H., Moon, J., Hanadari-Levy, A., Ophir, A.G., 2022. Synergistic consequences of early-life social isolation and chronic stress impact coping and neural mechanisms underlying male prairie vole susceptibility and resilience. Front. Behav. Neurosci. 16. https://doi.org/10.3389/fnbeh.2022.931549.

Schiller, M., Azulay-Debby, H., Boshnak, N., Elyahu, Y., Korin, B., Ben-Shaanan, T.L., Koren, T., Krot, M., Hakim, F., Rolls, A., 2021. Optogenetic activation of local colonic sympathetic innervations attenuates colitis by limiting immune cell extravasation. Immunity 54, 1022–1036.e8. https://doi.org/10.1016/J.IMMUNI.2021.04.007.

Schmidt, C., Skandali, N., Gleesborg, C., Kvamme, T.L., Schmidt, H., Frisch, K., Møller, A., Voon, V., 2020. The role of dopaminergic and serotonergic transmission in the processing of primary and monetary reward. Neuropsychopharmacology 45, 1490–1497. https://doi.org/10.1038/s41386-020-0702-3.

Schroeder, H.W., Cavacini, L., 2010. Structure and function of immunoglobulins. J. Allergy Clin. Immunol. 125, S41–S52. https://doi.org/10.1016/j.jaci.2009.09.046.

Shangase, K.B., Magwai, T., Oginga, F.O., Xulu, K.R., Mpofana, T., 2022. Effectiveness of double-hit model (Post-Weaning Social Isolation and NMDA Receptor Antagonist) in the development of schizophrenic like symptoms on rodents: a protocol for a systematic review. NeuroSci 3, 111–118. https://doi.org/10.3390/neurosci3010009.

Sladjana, D., Ljubica, G., 2005. Activity of pituitary-adrenal axis in rats chronically exposed to different stressors. Acta Vet. (beogr.) 55, 121–129. https://doi.org/10.2298/AVB0503121D.

Smith, K.J., Gavey, S., RIddell, N.E., Kontari, P., Victor, C., 2020. The association between loneliness, social isolation and inflammation: a systematic review and meta-analysis. Neurosci. Biobehav. Rev. 112, 519–541. https://doi.org/10.1016/j.neubiorev.2020.02.002.

Sorski, L., Melamed, R., Matzner, P., Lavon, H., Shaashua, L., Rosenne, E., Ben-Eliyahu, S., 2016. Reducing liver metastases of colon cancer in the context of extensive and minor surgeries through β-adrenoceptors blockade and COX2 inhibition. Brain. Behav. Immun. 58, 91–98. https://doi.org/10.1016/j.bbi.2016.05.017.

Steptoe, A., Shankar, A., Demakakos, P., Wardle, J., 2013. Social isolation, loneliness, and all-cause mortality in older men and women. Proc. Natl. Acad. Sci. 110, 5797–5801. https://doi.org/10.1073/pnas.1219686110.

Su, A., T, W., S, B., H, L., Ka, C., D, B., J, Z., R, S., M, H., G, K., Mp, C., Jr, W., Jb, H., 2004. A gene atlas of the mouse and human protein-encoding transcriptomes. Proc. Natl. Acad. Sci. U. S. A. 101. https://doi.org/10.1073/pnas.0400782101.

Sumis, A., Cook, K.L., Andrade, F.O., Hu, R., Kidney, E., Zhang, X., Kim, D., Carney, E., Nguyen, N., Yu, W., Bouker, K.B., Cruz, I., Clarke, R., Hilakivi-Clarke, L., 2016. Social isolation induces autophagy in the mouse mammary gland: link to increased mammary cancer risk. Endocr. Relat. Cancer 23, 839–856. https://doi.org/10.1530/ERC-16-0359.

Sun, M., Choi, E.Y., Magee, D.J., Stets, C.W., During, M.J., Lin, E.-J.-D., 2014. Metabolic Effects of Social Isolation in Adult C57BL/6 Mice. Int. Sch. Res. Not. 2014, 1–9. https://doi.org/10.1155/2014/690950.

Tan, M., Shallis, A., Barkus, E., 2020. Social anhedonia and social functioning: Loneliness as a mediator. PsyCh J. 9, 280–289. https://doi.org/10.1002/pchj.344.

Taugher, R.J., Lu, Y., Wang, Y., Kreple, C.J., Ghobbeh, A., Fan, R., Sowers, L.P., Wemmie, J.A., 2014. the bed nucleus of the stria terminalis is critical for anxiety-related behavior evoked by CO2 and acidosis. J. Neurosci. 34, 10247. https://doi.org/10.1523/JNEUROSCI.1680-14.2014.

Uchino, B.N., Trettevik, R., Kent de Grey, R.G., Cronan, S., Hogan, J., Baucom, B.R.W., 2018. Social support, social integration, and inflammatory cytokines: a meta-analysis. Health Psychol. 37, 462–471. https://doi.org/10.1037/hea0000594.

Umberson, D., Lin, Z., Cha, H., 2022. Gender and social isolation across the life course. J. Health Soc. Behav. 63, 319–335. https://doi.org/10.1177/00221465221109634.

Verza, F.A., Valente, V.B., Oliveira, L.K., Kayahara, G.M., Crivelini, M.M., Furuse, C., Biasoli, É.R., Miyahara, G.I., Oliveira, S.H.P., Bernabé, D.G., 2021. Social isolation stress facilitates chemically induced oral carcinogenesis. PLOS ONE 16, e0245190.

Villano Bonamin, L., Barbuto, J.A.M., Malucelli, B.E., 2001. Effects of social isolation on ehrlich tumor growth and tumor leukocyte infiltration in mice: evidence of participation of the submaxillary salivary gland. Neuroimmunomodulation 9, 313–318. https://doi.org/10.1159/000059388.

Vitale, E.M., Smith, A.S., 2022. Neurobiology of Loneliness, Isolation, and Loss: Integrating Human and Animal Perspectives. Front. Behav. Neurosci. 16.

Wang, F., Gao, Y., Han, Z., Yu, Y., Long, Z., Jiang, X., Wu, Y., Pei, B., Cao, Y., Ye, J., Wang, M., Zhao, Y., 2023. A systematic review and meta-analysis of 90 cohort studies of social isolation, loneliness and mortality. Nat. Hum. Behav. 7, 1307–1319. https://doi.org/10.1038/s41562-023-01617-6.

Wang, Y.-C., Ho, U.-C., Ko, M.-C., Liao, C.-C., Lee, L.-J., 2012. Differential neuronal changes in medial prefrontal cortex, basolateral amygdala and nucleus accumbens after postweaning social isolation. Brain Struct. Funct. 217, 337–351. https://doi.org/10.1007/s00429-011-0355-4.

Wang, H.-T., Huang, F.-L., Hu, Z.-L., Zhang, W.-J., Qiao, X.-Q., Huang, Y.-Q., Dai, R.-P., Li, F., Li, C.-Q., 2017. Early-life social isolation-induced depressive-like behavior in rats results in microglial activation and neuronal histone methylation that are mitigated by minocycline. Neurotox. Res. 31, 505–520. https://doi.org/10.1007/s12640-016-9696-3.

Weintraub, A., Singaravelu, J., Bhatnagar, S., 2010. Enduring and sex-specific effects of adolescent social isolation in rats on adult stress reactivity. Brain Res. 1343, 83–92. https://doi.org/10.1016/j.brainres.2010.04.068.

Winter, J., Jurek, B., 2019. The interplay between oxytocin and the CRF system: regulation of the stress response. Cell Tissue Res. 375, 85–91. https://doi.org/10.1007/s00441-018-2866-2.

Xia, N., Li, H., 2018. Loneliness, social isolation, and cardiovascular health. Antioxid. Redox Signal. 28, 837–851. https://doi.org/10.1089/ars.2017.7312.

Yang, Y.C., Li, T., Frenk, S.M., 2014. Social network ties and inflammation in U.S. Adults with Cancer. Biodemography Soc. Biol. 60, 21–37. https://doi.org/10.1080/19485565.2014.899452.

Yu, B., 2023. Social disconnection and mortality: new evidence for old truths. Trends Cogn. Sci. 27, 890–891. https://doi.org/10.1016/j.tics.2023.08.001.

Zhou, K., Zhu, Y., 2019. The paraventricular thalamic nucleus: a key hub of neural circuits underlying drug addiction. Pharmacol. Res. 142, 70–76. https://doi.org/10.1016/j.phrs.2019.02.014.